Adv Polym Sci (2008) 219: 107–171
DOI 10.1007/12_2008_146
© Springer-Verlag Berlin Heidelberg
Published online: 20 May 2008

Functional Self-Assembled Nanofibers by Electrospinning

A. Greiner · J. H. Wendorff (✉)

Department of Chemistry and Center of Material Science, Philipps-University, 35032 Marburg, Germany
wendorff@staff.uni-marburg.de

Abstract Electrospinning constitutes a unique technique for the production of nanofibers with diameters down to the range of a few nanometers. In strong contrast to conventional fiber producing techniques, it relies on self-assembly processes driven by the Coulomb interactions between charged elements of the fluids to be spun to nanofibers. The transition from a macroscopic fluid object such as a droplet emerging from a die to solid nanofibers is controlled by a set of complex physical instability processes. They give rise to extremely high extensional deformations and strain rates during fiber formation causing among others a high orientational order in the nanofibers as well as enhanced mechanical properties. Electrospinning is predominantly applied to polymer based materials including natural and synthetic polymers, but, more recently, its use has been extended towards the production of metal, ceramic and glass nanofibers exploiting precursor routes. The nanofibers can be functionalized during electrospinning by introducing pores, fractal surfaces, by incorporating functional elements such as catalysts, quantum dots, drugs, enzymes or even bacteria. The production of individual fibers, random nonwovens, or orientationally highly ordered nonwovens is achieved by an appropriate selection of electrode configurations. Broad areas of application exist in Material and Life Sciences for such nanofibers, including not only optoelectronics, sensorics, catalysis, textiles, high efficiency filters, fiber reinforcement but also tissue engineering, drug delivery, and wound healing. The basic electrospinning process has more recently been extended towards compound co-electrospinning and precision deposition electrospinning to further broaden accessible fiber architectures and potential areas of application.

Keywords Co-electrospinning · Electrospinning · Fiber architectures · Functions and applications · Nanofibers · Nonwovens · Precision electrospinning

1 Introduction

Spider webs are impressive for their complex architecture that gives rise to specific functions and in particular for their high performance ultrafine functionalized fibers from which the webs are constructed [1]. Several different types of silk are being used in web construction, including a “sticky” capture silk or “fluffy” capture silk, depending on the type of spider. Silk obtained

from cocoons made by the larvae of the silkworm Bombyx mori has a shimmering appearance which originates from the triangular prism-like structure of the fibers. This allows silk cloth to refract incoming light at different angles. Silk fibers possess highly impressive mechanical properties, in particular a high ductility, related to intrinsic structural features again being ultrafine in nature. Nature proves by these examples and many more not discussed here to be extremely efficient in creating functional materials in the shape of fine fibers.

This also holds for natural fibers such as cotton, wool, hairs, etc. [2]. These fibers are not as small in fiber diameter as the ones discussed above yet they are constructed in a highly complex hierarchical way which provides them not only with unique mechanical properties but also with another set functions which make them of interest for various types of applications. The diameter of such natural fibers may well be in the 10–20 μm range and above; human hair, for example, typically has a diameter around 50 μm. Strong correlations exist between a variety of functions displayed by natural fibers and their molecular and supermolecular structure devised by nature. Natural fibers composed of silk, wool, or cotton are used predominantly for textile applications providing functions such as thermal insulation, wind resistance, exchange of water vapor, etc., but they also contribute in unique ways in fashion design which frequently relies on the optical effects of silk produced by the prism-shaped fibers.

Man-made fibers, composed of materials such as polyamides or polyethylene terephthalate and produced via synthetic routes, have to a significant extent replaced natural fibers in textiles. They are advantageous, because they are cheaper to produce and easier to process, dye, or introduce high strength and stiffness in a controlled way [3]. Yet, to a certain extent, they miss quite a number of functions that are beneficial for textile applications and which are displayed by natural fibers. Wearing a shirt made purely from polyamide on a hot humid day makes the difference between textiles for example, from cotton and from man-made fibers very obvious. One major reason besides a chemical composition that is different from the one of the natural fibers discussed above is that their internal molecular and supermolecular structures tend to be rather simple. Solid fibers with constant composition and constant structural features along the cross section are characteristic of man-made fibers. Hollow fibers and also fibers with cross-sectional shapes that differ from the circular one have been produced, yet nevertheless such architectures are far from the complex ones displayed by nature [4]. Furthermore, specific microfibers have been produced along various ways, to enhance among other things, textile properties. A further strong reduction of the diameter of fibers used in textiles would at least greatly enhance thermal insulation, wind resistance, moisture absorption, exchange of vapor etc. It even seems possible that complex fiber morphologies may become accessible through control by confinement effects.

In fact, the application of man-made fibers is not only restricted to textiles. Fibers play a major role in the reinforcement of thermoplastic and thermoset polymer matrices for high-end applications [3, 5]. Reinforcement of high end elements of ships, trains, and airplanes are well known, but fiber reinforced materials can also be found in day to day appliances. As far as fiber reinforcement is concerned, the important parameters are the axial ratio, which should be well above 100 to 1000 (thus the use of fibers), and the enhanced stiffness and strength of the fiber combined with a good mechanical coupling to the matrix. Fiber reinforcement is in the majority of cases not done with natural fibers [2, 3], although such approaches are being considered more and more for ecological reasons, but is conventionally done by using very specific synthetic fibers (such as carbon fibers produced among others via precursor polymer polyacrylonitrile (PAN) fibers or Kevlar fibers, produced from lyotropic polymer solutions) [3]. Fiber reinforcement could stongly benefit from fibers much smaller in diameter, even at the same magnitudes of stiffness and strength, since the length could be reduced at constant axial ratio compared to thicker fibers reducing thus rupture during polymer processing. In addition, fibers small in diameter compared to the wavelength of light would not cause turbidity in otherwise transparent matrices. It follows that the mechanical coupling between matrix and fibers will be enhanced, and, thus, the ductility, due to the much larger internal surface areas.

A further area for the application of fibers, again predominantly of man-made fibers, concerns filters for either gas or fluid filtrations including coalescer filters [6]. The chemical, thermal, and mechanical stability of the fibers together with the costs to produce the fibers are important features, but the absolute magnitude of the diameter of the fibers is of particular importance. The diameter determines the size of the pores provided by the filters and thus the size of the impurities to be filtered out. The reduction to fiber diameters within the nanometer range will affect the flow pattern around the fibers significantly and should strongly enhance the filter efficiency with respect to smaller scale impurities in the air, in gasoline, etc. The specific surface area acting as adsorption site also increases strongly as the diameter is reduced.

The discussion about fiber applications in the areas of textiles, fiber reinforcement, and filters has made it apparent that these areas would benefit to a great extent from a further strong reduction of the fiber diameters by several orders of magnitude well into the nanometer range. The low value of the diameter and small nonwoven pore sizes, as well as the huge surface area which goes along with small fiber diameters, are key factors in such applications. Yet, it is obvious that the extremely small diameter is just one side of the coin. Further features are the onset of confinement effects for structural features and properties and the increasing truly 1-dimensional nature of the fibers as the diameter decreases. The potential for rapid diffusional processes into and out of the fiber characteristic of nanoscalar dimensions, the close resemblance in architecture of electrospun fibers, and the fibrillar extracellular matrix in living systems are

further specific features favorable to specific applications. It may, of course, be necessary for such fibers to carry functional units such as chromophores, catalysts, sensor molecules, quantum dots, drugs, or bacteria depending on the application in mind, and they may have to be composed of organic, inorganic materials, or corresponding hybrids.

Conventional processing techniques will not be able to yield such extremely fine functionalized fibers. This inability also holds for melt blowing and similar special techniques [7, 8]. The technique of choice is electrospinning. Prior to the year 2000 electrospinning was the domain of a few specialists; the average number of papers published per year on this topic was well below 20. This situation has changed dramatically in the last few years. In 2007, more than 500 papers have been published on electrospinning. It is estimated that more than 200 research groups in academia and industry work currently on this topic, and the number of conferences and conference sessions devoted to electrospinning is continuously increasing. Electrospinning has become a widely appreciated nanostructuring technique in academia and industry and, in fact, has a lot to offer [9–13].

Basically it allows production of nanofibers with diameters down to a few nanometers from a broad range of polymers. Yet, due to the unique self-assembly processes happening in electrospinning, it is a highly versatile technique in terms of the materials that can be spun to nanofibers, the control of their morphology, their surface topology, as well as the properties of the fibers and nonwovens composed of them. Figure 1 illustrates the broad range of fiber architectures available from electrospinning including thin smooth fibers, porous fibers, and fibers with fractal surface structures, with spindle-type disturbances, ribbonlike fibers or odd-shaped fibers, such as "barbed" nanowires.

A multitude of functions can be incorporated into these fibers, and an extremely broad range of potential applications exists in which electrospun fibers can make major contributions. These include not only textile, filter and mechanical reinforcement applications but also extend to tissue engineering, drug delivery, wound healing, sensorics, optoelectronics, catalysis, and many more applications. The progress achieved in electrospinning in a time span covering less than one decade, coupled with the strong impact it has made and continues to make on Material and Life Science are unique features. A set of review articles have recently been published that provide an insight into the vast opportunities afforded by electrospinning [9–13].

It is of particular importance for the discussions that follow to point out that fiber formation processes in electrospinning differ fundamentally from the ones in conventional technical approaches, such as extrusion and subsequent elongation, melt blowing, or even techniques exploiting converging flow, which all involve mechanical forces and geometric boundary conditions [14, 15]. In melt or solution extrusion the shape and diameter of the die, as well as mechanical forces inducing specific draw ratios and drawing speeds, to a major extent

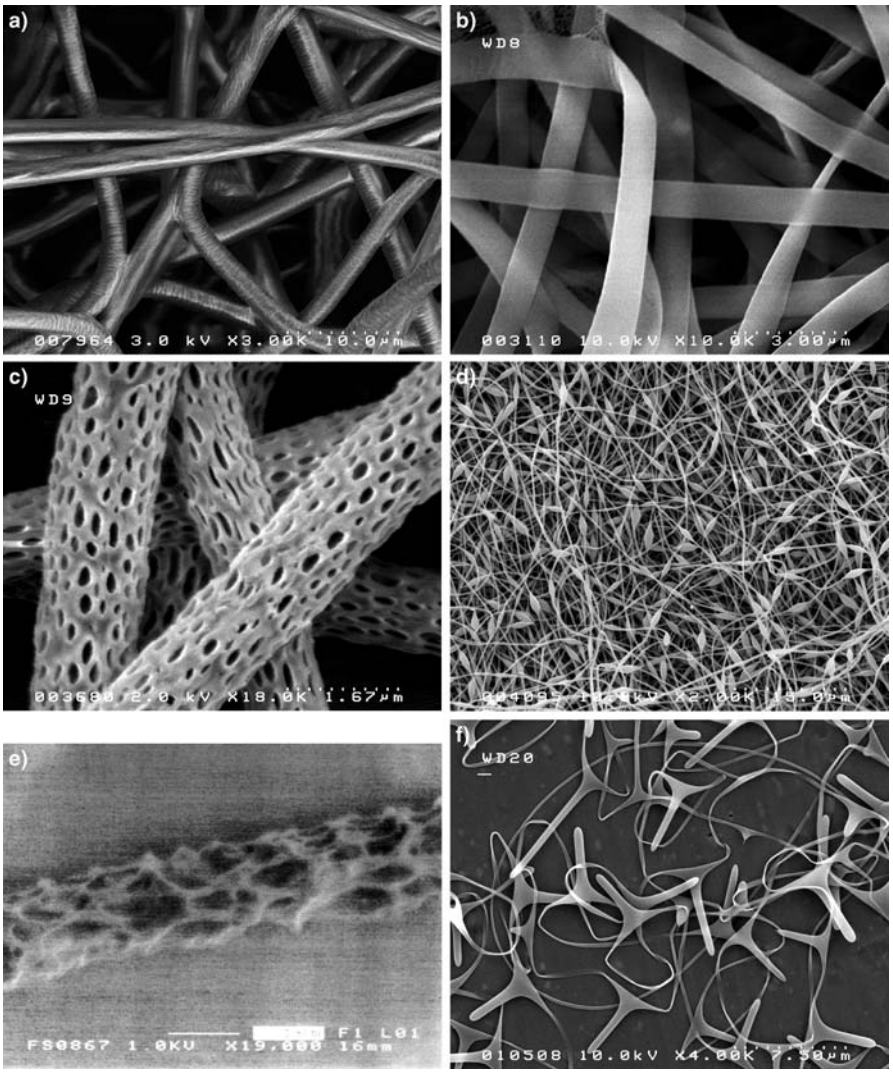

Fig. 1 Nanofiber architectures available from electrospinning: **a** Thin smooth fibers with circular cross section (PA 6), **b** Ribbonlike fibers (PA 6) **c** Porous fibers (PLA) and **d** Fibers with spindle-type disturbances (PAN), **e** Fibers with fractile shape (PLA), **f** "Barbed" nanofibers (PVA)

determine dimensional and structural properties of the resulting fibers. Fiber formation is thus controlled by mechanical deformation processes to which the original solution or melt are subjected. In an extension of the extrusion technique, multicomponent fibers consisting of segments of different polymers can be fabricated by extrusion. The subsequent preparation of fine fibers is induced by splitting up the fiber by treatment with, for example, water jets [8]. The melt

blowing process is a technically advanced process leading to fibers with diameters below 500 nm. In the melt-blown technology polymer melts are pumped through an array of nozzles. In the process, the formation of fibers from the melt is obtained via cooling in a strong countercurrent of air again imposing specific mechanical forces.

Another interesting approach is the exploitation of converging flow to first produce droplets, as in electrospraying, but in specific cases, including nanofibers [14, 15]. The concept in one particular setup is to start from a fluid layer arrangement composed of two immiscible fluids, one of which serves as processing fluid and the other constituting the material to be processed to fibers. These fluid layers are sucked by mechanical forces through a die which imposes a converging flow. For slow sucking speeds only the upper sacrificial fluid layer is subjected to the converging flow, yet at higher speeds the lower fluid layer is also sucked in, yielding a compound jet with the sacrificial material forming the outer shell. The fluid core fiber is subsequently either subjected to a breakup, yielding droplets, or solidifies, yielding fibers with diameters well below the micrometer range. Using three layer arrangements, core shell fibers or hollow fibers can be produced in this way. Again fiber formation is controlled in this approach by mechanical forces as in conventional extrusion, although the strong correlation existing between die diameter and final fiber diameter is relaxed to a certain extent.

Fiber formation in electrospinning differs strongly from the formations occurring in the approaches discussed so far, since self-assembly processes dominate in electrospinning (which will become apparent in detail as the theory of electrospinning is explained below). Features that are basically governed by self-assembly processes induced by specific electrostatic interactions of elements of the original source droplet or similar geometries from which fiber formation starts include: the evolution of the final diameter of the nanofibers resulting from electrospinning, the intrinsic orientational order, the morphology, the cross-sectional shape, gradients along the cross section, specific phase morphologies, as well as the distribution of solid particles dispersed within the fiber, undulations of the fiber diameter, and droplets arranged along the fibers in a regular fashion.

In the case of supramolecular structure formation self-assembly is known to be controlled by specific, generally attractive, forces such as hydrogen bonding, charge transfer interactions, etc. [16, 17]. Self-assembly in electrospinning, on the other hand, is controlled by Coulomb interactions between charged elements of the fluid body. Self-assembly follows the general Earnshaw theorem of electrostatics according to which it is impossible to prepare stable fluid structures such as stable fluid jets in which all elements interact only by Coulomb forces [18, 19]. Charges located within the fluid jet, in the case considered here, move the polymer elements to which they are attached along complex pathways in such a way that the Coulomb interaction energy is minimized. Droplet deformation, jet initiation, and, in particular, the bending instabilities that to

a major extent control fibers' properties are apparently predominantly controlled by this kind of self-assembly principle. Simple as well as highly complex fiber architectures, the deposition of flat fibers, of fibers with vertical protrusions, and splayed fibers can be considered as a manifestation of the variety of self-assembly processes happening in electrospinning (see examples in Fig. 1). Keeping this general theorem in mind it should be possible to come up with completely novel fiber architectures – Fig. 1f may serve as an example – and thus novel functions in the future. In view of this very specific character of fiber formation via electrospinning, it seems reasonable to first consider the electrospinning process in detail, both from an experimental and theoretical point of view, before embarking on the Material Science aspects and application sides of electrospinning.

2
Nature of the Electrospinning Process

2.1
Experimental Setups

At first glance, electrospinning gives the impression to be a very simple and therefore easily controllable technique to produce fibers with dimensions down into the nanometer range. In electrospinning on a simple laboratory scale, a polymer solution or melt is pumped through a thin capillary acting as a die with inner diameters in the range of some 100 μm (Fig. 2). The die may simultaneously serve as an electrode to which high electric fields in the range of typically 100 to 500 kV/m are applied. The distance to the counter electrodes typically amounts to 10 up to 25 cm in laboratory systems and currents flowing during electrospinning are in the range of some 100 nanoamperes up to several microamperes. The substrate on which the electrospun fibers are collected is either the counter electrode material itself or specific substrates selected in view of the target application. It may be brought into electric contact with the counter electrode but it can also be on a different potential. Frequently a top-down arrangement of the die/electrode and the counter electrode is used (Fig. 2), but in principle electrospinning can be carried out with the jet flowing from bottom to top, top to bottom, and horizontally.

To discuss other types of electrospinning devices one has to take into account the fact that electrically initiated jets will generally not start easily on flat fluid surfaces but rather at protrusions [20, 21]. Such protrusions can have the shapes of pending droplets located at the tip of syringe-like dies, an approach used typically in laboratory style electrospinning device, or of sessile droplets positioned on flat solid surfaces [21]. In more technically oriented spinning devices such protrusions may also be formed via metal spikes arranged along

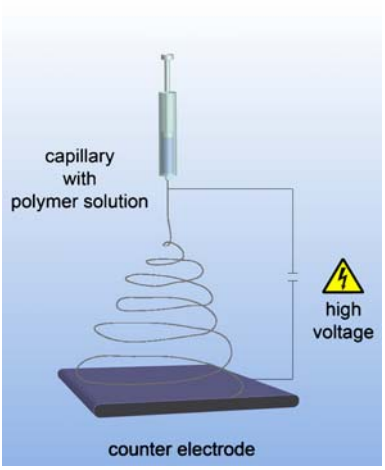

Fig. 2 Electrospinning device, laboratory scale, schematic representation

metal wires or along metal cylinders immersed into or carrying the spinning fluid. The spikes thus assume two roles: they act as solution feeding elements as well as initiation elements. Another unique approach towards the creation of protrusion on fluid surfaces consists in inducing statistical surface roughness modulations, for instance via superparamagnetic particles immersed in the spinning solution via their interactions with magnetic fields [22]. Magnetic fields tend to induce spike structures for such systems. Many more approaches along this line seem feasible and possibly necessary if one intends to scale up the production rate considerably. Multiple die arrangements have been used to this end with limited success. One reason is that the equally charged jets emanating from these dies tend to reject each other and that such an arrangement can only be optimized to deposit fibers on a substrate in a completely homogeneous way with great difficulties.

2.2 Experimental Observations on Fiber Formation

Experimental observations employing, for example, high-speed video analysis reveal for electrospinning devices of the kind introduced above (i.e., for laboratory scales) a sequence of complex fiber forming processes resulting finally in the deposition of extremely fine fibers, of nanofibers, on the counter electrode or substrates such as glass, silica, filter paper or textiles located on top of the counter electrode. The first step towards fiber formation consists in the deformation of fluid drops emerging from the die by the interaction of the applied field with the charged fluid [23] (Fig. 3). With increasing electric field, the shape of the droplet becomes increasingly prolate and approaches a con-

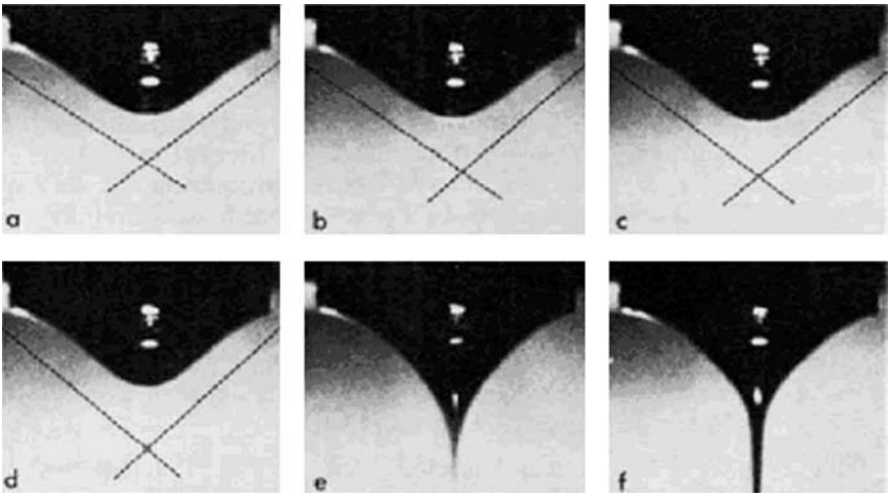

Fig. 3 Deformation of a pending droplet by electric fields [23] (see discussion below)

ical shape with the half angle of the cone assuming values of the order of 30° (Fig. 3a–d). The cone is furthermore characterized by a tip with a very low radius of curvature, well below 1 μm, and thus not readily resolvable by optical means [19–21].

A fluid jet emanates from this tip as a critical electric field is surpassed (Fig. 3e and f). This jet moves towards the counter electrode in a linear fashion for a short distance amounting typically to several centimeters. At the end of the straight path unstable bending motions occur with growing amplitudes and the jet begins to follow a spiralling and looping path in space (Fig. 4).

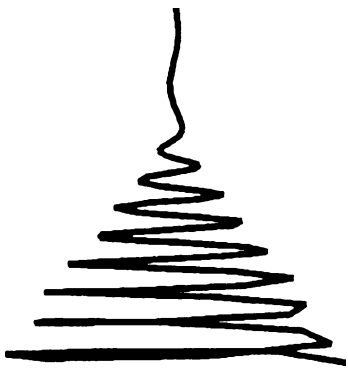

Fig. 4 Path of a fluid jet in electrospinning, schematic representation as adapted from [19]

2.2.1
The Straight Path of the Jet

In the following, experimental observations on dynamics related to this straight path of the jet collected from tracer particle tracking techniques based on high-speed photography will be discussed [13, 24]. The fluid jet is found to experience a very strong acceleration as it leaves the die going up to 600 m/s^2, which is close to two orders of magnitude larger than the acceleration coming from gravitational forces. Gravitational forces thus play no significant role in electrospinning. This is the reason why top-down, bottom-up, and other types of die/counter electrodes work similarly. The velocity of the jet amounts typically to 3–5 m/s at the end of the straight part of the jet. Further characteristic values are a strain rate which goes up to values of the order of 1000 s^{-1} and an elongational deformation approaching values of up to 1000. An important fact is that an increase of the voltage causes on one side the jet diameter to increase, whereas with the acceleration, the jet velocity as well as the strain rates decrease with significantly increased voltage. The interpretation is that a lower voltage gives rise to a lower feeding rate of the fluid, which in turn causes the jet to be thinner thus allowing larger surface charge densities. The surface charge density is a controlling parameter in fiber formation via electrospinning.

The strain rates characteristic for the straight part of the jet are sufficiently large enough to induce chain extension. Arguments on requirements to be met by the strain rate relative to the hydrodynamic relaxation in order to induce chain orientation have been put forward by de Gennes [25]. These lead to the conclusion that the product of the viscoelastic relaxation time and the strain rate should be larger than 0.5 for the induction of chain extensions. In fact, this product goes up to 50 in the straight path of the jet and again it goes down significantly – to 30 and below – as the electric field is increased, e.g., from approximately 50 to approximately 70 V/mm. It is thus not surprising that, in fact, birefringence has been observed for this part of the jet, which is still, of course, fluid. A further observation is that the birefringence tends to be stronger at the surface of the jets. Some reasons are that the surface charges are located just there, that polymer chains located at the surface possess lower degrees of freedom which tends to make them more susceptible to deformation, and that the surface layers tend to have a higher concentration of polymer chains due to the evaporation of the solvent.

2.2.2
The Looping Part of the Jet

At some distance away from the die the jet is no longer able to follow a straight path in the direction of the counter electrode. It bends, turns sideways, and begins to perform spiralling, looping motions. In each loop the jet

becomes thinner and elongated as the loop diameter increases. The envelope of these loops, which is apparent in electrospinning to the naked eye, resembles a cone with its opening oriented towards the counter electrode. This type of instability – bending (also known as whipping instability) – repeats itself in a self-similar fashion on a smaller and smaller scale as the jet diameter is reduced, contributing to a further reduction of the jet diameter. Finally, the jet is so thin or the fiber becomes so stiff that the bending instability can no longer govern the fiber formation process. The deposition of solidified nanofibers onto the counter electrode or substrates located on top of the counter electrode is the final step in electrospinning. The radius of the envelope cone which typically assumes a value of the order of 10 up to 15 cm over a characteristic distance between the die and the counter electrode of approximately 10 to 15 cm also controls the radius of the planar nonwoven, which is deposited in the plane of the counter electrode of similar magnitude.

Nonwovens are defined in this context as textiles which are neither woven nor knit, for example felt. Nonwoven fabric is typically manufactured by putting small fibers together in the form of a sheet or web. Note that in electrospinning the deposition texture depends on the electrode configurations. In the case of planar counter electrodes, a planar texture results, i.e., the fibers are randomly oriented within the plane of the substrate as shown in Fig. 5 for the case of fibers from polyvinyl acetate (PVA). A highly porous nonwoven results with the sizes of the pores, which is on the average much larger than the diameter of the fibers.

Both the elongation and thinning of the fiber within the linear pathway and within the looped pathway are accompanied by solvent evaporation, contributing also to jet diameter thinning and to the final diameter of the solid nanofibers deposited on the counter electrodes. Again using high-speed video analysis and laser Doppler velocimetry, the magnitudes of the total elongation of the jet during electrospinning, the deformation rate, and the speed with

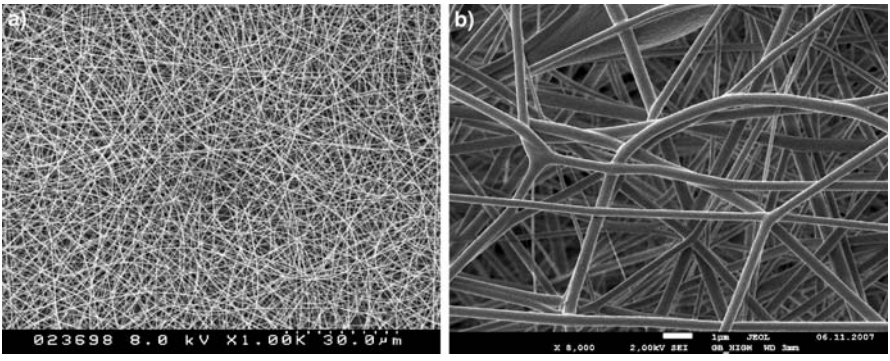

Fig. 5 Nanofiber nonwoven obtained by electrospinning shown at two different magnifications

which the fibers are deposited on the counter electrode can be estimated [26]. The total time which a fluid element experiences within the fiber formation process from leaving the die until becoming deposited on the counter electrode as element of the solid nanofiber is estimated to be approximately 0.2 s. The overall draw ratio is estimated to be of the order of 10^5 and the overall strain rate to be of the order of $10^5\ s^{-1}$ [13, 19]. These are extremely high values reflecting the reduction of the jet diameter from around 100 μm down to 100 nm and below in a very short time (well below a second), when taking into account the evaporation of the solvent and the corresponding reduction in diameter. It is obvious that chain molecules tend to become highly oriented in the jet during electrospinning and that this should show up in the orientational order within the final solid fibers as well as in the crystal morphology. Furthermore, such a strong mechanical deformation should also be reflected in the stiffness and strain of the fibers (these topics will all be discussed later in some detail).

In general solid fibers are deposited on the counter electrodes despite the short fiber formation times well below a second and even if solvents with high boiling points, such as water, are used for the spinning solutions. Yet, depending on the relative humidity, high solvent concentrations, and the use of polymer materials with glass transition temperatures close to or below room temperature, soft fibers are deposited giving rise to partial coalescence effects (Fig. 6a). Coalescence processes set in whenever two soft fibers within the fiber network resulting from electrospinning come in close contact or whenever two such nanofibers cross each other, respectively [89]. Coalescence of fluid droplets in close contact and also of elliptically deformed droplets have been studied widely experimentally as well as on a theoretical basis, yet it seems that such calculations were not extended to fiber coalescence in nonwovens.

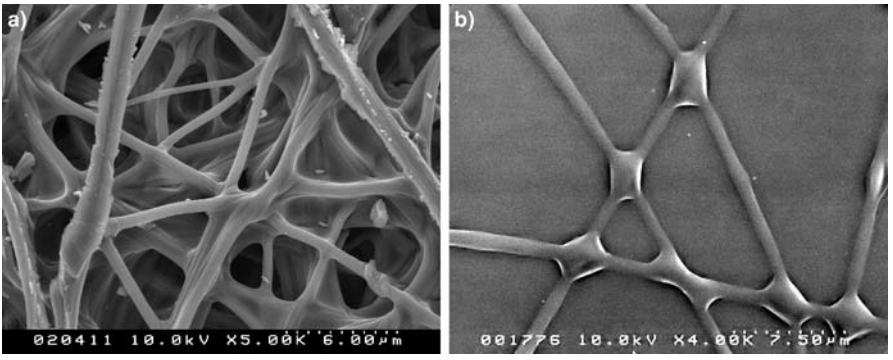

Fig. 6 Coalescence of soft nanofibers. **a** Directly during deposition of soft fibers in electrospinning of cellulose acetate, **b** Result of annealing of polylactide nanofibers at enhanced temperatures [89]

The observation is that coalescence sets in at the contact points of the nanofibers yielding distinct geometries for the junction points, which depend on the angle with which the fibers contact each other and also on the diameters of the two fibers in question, i.e., whether they have a similar diameter or different diameters. The common feature of these geometries is that the disrupted directional variations characteristic of the crossing of two fibers that have still retained their circular cross section is replaced by geometries characterized by more continuous variations of the curvature. The coalescence figures that result during electrospinning are frequently kinetically controlled, as governed by the simultaneous processes of jet deposition and solidification due to solvent evaporation. To obtain coalescence figures corresponding more closely to the equilibrium one may anneal electrospun nanofibers crossing each other at elevated temperatures above the glass or melting temperatures for some minutes [89]. The geometries which result are displayed in Fig. 6b. They quite obviously correspond to low surface free energy configurations spontaneously produced by the tendency of the system to approach the lowest state of surface free energy. Such coalescence processes lead to a mechanical cross-linking of the nonwovens. Such features may be of interest for a set of applications including filter, textile, or tissue engineering applications. Cross-linking may enhance the stiffness and strength of the nonwovens, and cross-linked nonwovens tend to keep their integrity even in the presence of mechanical forces.

It is helpful at the end of this section to compare specific textile fiber properties of conventionally produced fibers with diameters in the micrometer range with fibers in the nanometer range that are produced by electrospinning. From one gram of polyethylene fibers, a total length of 13 km can be produced if the fiber diameter is 10 μm, but a length of 130 000 km if the diameter is 100 nm. In the first case the specific surface, which is the surface given in m^2 per gram fibers, amounts to about 0.4 m^2/g while in the second case it amounts to 40 m^2/g. In fiber technology the unit denier is often used of as a measure of fiber fineness. It determines the mass of a fiber with a length of 9000 m. For a 10 μm fiber the fineness amounts to 1 denier, for a 100 nm fiber the fineness is 10^{-4} denier. Further properties of nanofibers made by electrospinning will be discussed later in some detail.

2.3
Theoretical Analysis

2.3.1
Droplet Deformation and Jet Initiation

The transition of a bulk fluid material – either a melt or a solution – into extremely fine fibers, i.e., nanofibers with diameters down to a few nm, possibly with unique morphological and topological features, involves a sequence of

complex deformation processes. These depend, on the one hand, on external parameters characteristic of the electrospinning technique itself (such as the applied field, the electrode configurations, or the feeding rate of the fluid to be spun) and, on the other hand, on intrinsic parameters characteristic of the spinning fluid itself (such as the surface free energy, the electric conductivity, and the viscous and elastic properties).

2.3.1.1 Droplet Deformation

The primary step in nanofiber formation involves the initiation of a fluid jet emanating from the spinning fluid due to its interaction with the electric field. This jet will in general not be initiated on flat fluid surfaces but rather at protrusions. Such protrusions can have the shapes, as previously discussed, of pending droplets located at the tip of syringe-like dies or of sessile droplets positioned on flat solid surfaces. They may also be formed via metal spikes arranged along metal wires or along metal cylinders encapsulated by the spinning fluid or even through statistical surface modulations induced by various means. Many more approaches along this line seem feasible.

The interactions of droplets/fluid protrusions with electric fields were considered in a set of papers going back as far as to the year 1882 concentrating predominantly on pendent and, to a lesser extent, on sessile droplets [27]. A frequent assumption is that the fluids to be spun such as polymer solutions or polymer melts tend to display an ionic conductivity to some degree. Within the electric field the anions or cations become nonuniformly distributed on the surface of the droplets in such a way that the surface becomes equipotential and the field inside the droplet zero. The general result of the theoretical analysis is that such droplets are deformed within the electrical field and display a stable critical shape even when close to a critical electric field beyond which jet formation occurs from the tip of the deformed droplet (Fig. 3). The shape should in principle be controlled by the equilibrium between the electric forces and surface tension as far as viscous and viscoelastic fluids are concerned, whereas nonrelaxing elastic forces may also affect the shape of the droplet. Yet, the papers on droplet deformation differ in the mathematical approaches taken and in their predictions on the shapes of the deformed droplets.

The interaction of fluid droplets with electric fields is a topic which was met with interest as long as 100 years ago. One motivation was the belief that the disintegration of water droplets in strong electric fields plays a major role in the formation of thunderstorms. In 1882 Rayleigh calculated the limited charge an isolated droplet can carry before it becomes unstable [27]. Using the same approach Zeleny analyzed the deformation of a droplet in an external electric field representing the shape of the droplet by a steroid [28]. Rayleigh subsequently argued that this approach is unsound for a droplet in

an external electric field and calculated the deformation of the droplet due to the balance between internal pressure, surface tension, and electric forces (assuming also a spheroid as the representative shape of a water droplet) [29]. One problem of the analysis is the field dependence of the shape of the charged droplet and vice versa so that approximations have to be introduced in the analysis of the balance of forces. One approach, for instance, is concerned with the balance just at the poles and the equator of the deformed droplet. To be able to consider not only droplet deformation but also the mechanics of jet formation additional assumptions had to be introduced, such as a power law scaling of the electric potential [13, 29]. Predictions of the treatment by Tailor are that the droplet assumes a prolate shape and becomes unstable if the ratio of the length to the equatorial diameter approaches 1.9. Furthermore, the droplet is predicted to approach a conical shape close to the critical field with a half angle of the cone of 49.3° at the tip of the droplet. One finds half angles significantly smaller than this value in experiment (Fig. 3).

The problem of the shape of droplets in electrical fields was therefore revisited in the context of electrospinning (in particular by Yarin et al. [20]). First, they pointed out the self-similar nature of the treatment by Taylor. Second, they stated that the likely shape of a droplet in electrospinning must be very close to a hyperboloid of revolution. They then looked for self-similar and non-self-similar solutions for the balance of electric and mechanical forces and the corresponding shapes for hyperboloidic liquid droplets. The self-similar approach turned out to fail whereas the non-self-similar approach yielded results in agreement with the experimental ones. Based on the hyperboloidic approach, they predicted that the stationary critical shape assumed by the droplet in the critical electric field can be represented by hyperboloids approaching a conical asymptotic with a half angle of 33.5°. For sessile droplets the experimental analysis yielded values for the half angle that were close to the tip of the droplet of about 37° decreasing to 30.5° at locations farther away from the tip. In fact, the half angle experimentally observed for pending droplets close to the tip amounts to 31° decreasing to 26° at locations on the droplet surface further removed from the tip. In all cases these values are closer to the ones predicted by the hyperboloidal approach as compared to the spheroidal approach. A further interesting result of this analysis was that the curvature of the deformed drop at its tip is very small, amounting to about 600 nm. It can thus not easily be analyzed by optical means.

2.3.1.2 Jet Deformation

A highly important step in electrospinning that controls the fiber diameter as well as the orientational order and mechanical properties of the resulting nanofibers via self-assembly steps is the onset and further evolution of the bending instabilities. These were consequently analyzed in some detail by

a set of theoretical approaches. It was pointed out by Yarin et al. that this feature in electrospinning and possibly other related phenomena seem to follow a very general theorem of electrostatics formulated by Earnshaw [18, 19]. According to this theorem it is impossible to prepare stable structures such as fluid jets in which all elements interact only by Coulomb forces. Charges located within the fluid jet, in our case, move the polymer material to which they are attached along complex pathways in such a way that the Coulomb interaction energy is minimized.

To be more specific even a simple linear arrangement of three equal charges arranged along a chain becomes unstable towards lateral deflections. Following this line of arguments Yarin et al. modeled the bending instabilities and the jet path resulting from them by a system of connected viscoelastic dumbbells with the beads in the dumbbells having masses and electrical charges representative of the charged polymer jet to be modeled [19]. The beads, in turn, interact among each other via springs and dashpots representing the mechanical interactions in the jet as well as its viscoelastic response towards the elongation during electrospinnning. The beads furthermore interact with each other by Coulomb forces since they carry charges. Finally, the interactions between the charged beads and the applied electric field are taken into account. Based on this straightforward model the evolution of the path of the fluid jet in the presence of bending perturbations was calculated. It turns out that the model provides a quite accurate description of the path of the jet, including the complex looping and spiraling motions (Fig. 4). This holds, for instance, not only for the conic envelop of the path within the bending instability range, but also for the magnitudes of the diameter reduction, total elongation, and deformation rate to which the jet is subjected.

This model, however, does not take into account the evaporation of the solvent during fiber formation or the onset of solidifications induced by the evaporation and the glass formation or crystallization, respectively. In fact, these processes affect the path of the jet to a considerable extent. The conic envelope representing the looping and spiraling of the jet in its bending mode is strongly extended both in the lateral and longitudinal directions as compared to the case neglecting evaporation and solidification. Further, the magnitudes of the total elongation and rate of elongation are affected as already discussed above [30]. The authors point out that details of the evaporation process and solidification process could not be taken into account since these details depend on the system studied, are actually unknown for most experimental systems, and have to be analyzed for the specific system of interest. Thus, the theory is able to give general estimates that definitely point into the right directions, as made obvious from a comparison between the experimentally observed features and the calculated ones. An interesting point of the theoretical analysis is that the formation of bending instabilities becomes

suppressed if the surface energy of the jet becomes sufficiently large, keeping all other spinning parameters constant [13].

The observation that electrospinning does not always give rise to fibers with uniform diameter, but rather – for specific operating parameters – to fibers displaying modulations of the diameter, droplets or spikes arranged along the fiber length, to the deposition simultaneously of fibers and droplets on the counter electrode, or even just of droplets (Fig. 7a,b) are indications that the electrospinning process is even more complex than discussed so far. Observations show that frequently droplets form along the length of the jet in its straight part and that the slender jet/droplet arrangement subsequently becomes subjected to bending motions. On the positive side, these observations point out in which way, by a suitable choice of spinning parameters, the range of nanofiber architectures can be considerably expanded, which might be beneficial for specific applications.

Through their theoretical approaches, Hohman et al. have investigated the richness of structure formation processes taking place in electrospinning going beyond the bending instability (such as the axisymmetric instability depicted in Fig. 8 in addition to the bending instability) [31–34].

In fact, they were able to predict first of all phase diagrams specifying for which spinning parameters which kind of structure formation process/type of instability is dominant, and they secondly specified operating diagrams for electrospinning in terms of the feeding rate of the spinning solution and the applied electrical field for given properties of the spinning fluids. Such diagrams (to be discussed in more detail below) allow selection of electrospinning parameter sets in such a way that the bending mode becomes dominant yielding smooth fibers with homogeneous fiber diameters. Yet, they also allow selection of these parameters in such a way that other types of instabilities take over yielding, e.g., fibers with droplets attached to them, thus corresponding to the electrospraying mode.

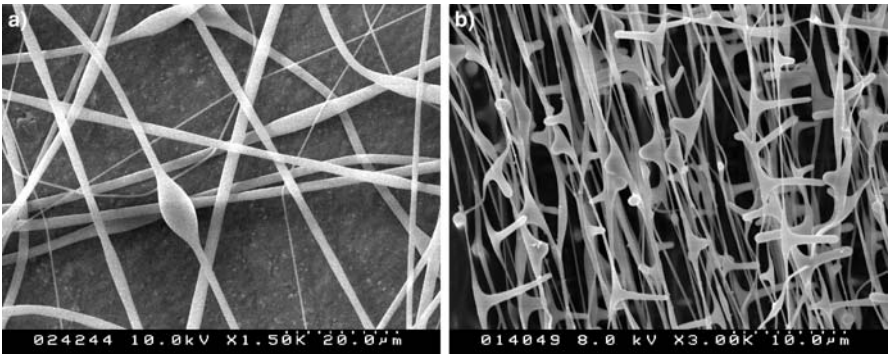

Fig. 7 Electrospun nanofibers: **a** With beads (PS) and **b** With spikes (barbed nanowires) along the fibers (PVA)

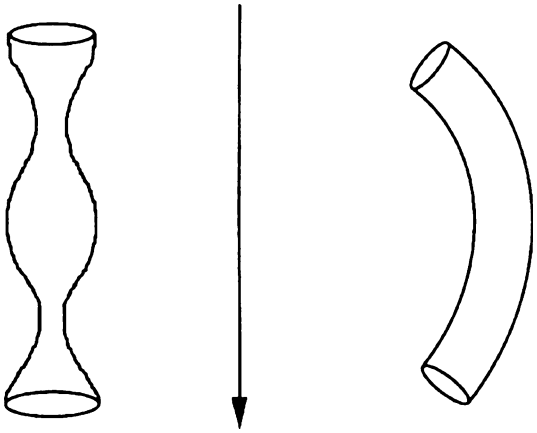

Fig. 8 Schematic sketch of an axisymmetric instability (*left*) and bending instability adapted from Shin et al. [33]

Hohman et al. based their theoretical analysis on classical hydrodynamics adapted to the particular case of long fluid cylindrical elements carrying charges and being located in an electric field – mimicking the jet in electrospinning [31–34]. Details of the theoretical analysis will not be spelled out in this contribution but should be explored in the respective papers. This contribution will rather concentrate on major predictions of interest for the experimentalist. In this context it is sufficient to point out that the treatment has to consider in addition to the conservation laws for the mass and the charges the presence of viscous dissipation, of electric forces arising from the coupling of the charged fluid elements to the electric field but also of gravitational forces. Electrostatic terms were thus introduced into the hydrodynamic equation. Furthermore, to facilitate the theoretical treatment and to adapt it to the situation of a long, slender fluid cylinder with a specific axial ratio expression for the flow velocity and electric field components (radial and tangential) were expanded in a Taylor series in powers of the aspect ratio of the slender fluid cylinder and introduced into the electro-hydrodynamic equations.

The theoretical analysis comprises two different steps:

(i) In the first step, the stability of this fluid electrically charged element is investigated at fixed charge density, surface tension, viscosity, and dielectric constant.
(ii) In a second step the treatment takes into account the fact that these properties vary along the jet as it moves from the die to the counter electrode.

The analysis first of all specifies the types of instabilities to which such a fluid element is subjected.

The first one is the electric counterpart of the classical Rayleigh instability known from uncharged fluid threads, already discussed above. This type of

instability is controlled by surface energy contributions, and it consists in the growth of diameter perturbations eventually causing a breakup of the long cylindrical element into individual isolated droplets. The presence of surface charges tends to reduce the effect of the controlling parameter surface energy on the growth of the instability. The instability becomes weaker with increasing electric fields and surface charges, respectively, and it becomes totally suppressed above a critical field for which the electric pressure coming from the surface charges exceeds the surfaces tension pressure. The critical field depends linearly on the surface tension and inversely on the radius of the jet. Furthermore, the analysis shows that this type of instability does not cause a breakup of the jet for the set of spinning parameters usually used in electrospinning. One exception is the situation in which the jet diameter becomes very small, close to its deposition on the counter electrode.

The second type of instability observed (also for slender fluid elements) causing a growth of diameter perturbations with a final breakup is totally controlled by charge contributions rather than by surface energy. In the case of the charge driven axisymmetrical instability, a statistic variance of the jet's radius causes a modulation of the surface charge density. This in turn generates tangential electrical forces that couple to the radius modulation and amplify it. The formation of beads is the end result of such a coupling loop. In fact, during electrospinning fibers on which drops along the fiber are aligned like pearls on a string can be observed for certain sets of spinning parameters (Figs. 7 and 8).

Finally, the theoretical analysis by Hohman et al. [31–34] yields not unexpectedly the bending instability discussed already in detail previously and called whipping instability in these papers. An important outcome of this theoretical analysis for experimentalists is the prediction of phase diagrams for the various instabilities and of operating diagrams specifying for which set of operating parameters electrospinning can be performed to produce the bending instability yielding homogeneous fibers respectively: the whipping or bending mode is enhanced if the local electrical field near the jet is dominated by its own charges, and it is suppressed if the local field is governed by the external tangential field (Fig. 9).

Figure 9 displays a characteristic operating diagram specifying the dominance of either the bending or the conductive axisymmetric instability as a function of the operating parameters flow rate of the spinning solution and applied field for given values of fluid parameters (such as the surface tension, viscosity, electric conductivity, and dielectric constant).

The general trends of such operating diagrams do not change significantly as the fluid properties are modified but rather just the absolute numbers vary. The operating diagram reveals which way the field and flow rate have to be controlled to yield the bending instability and thus ensure stable electrospinning of smooth nanofibers. In experiments, one has to determine the fluid parameters mentioned above and then one should be able to optimize elec-

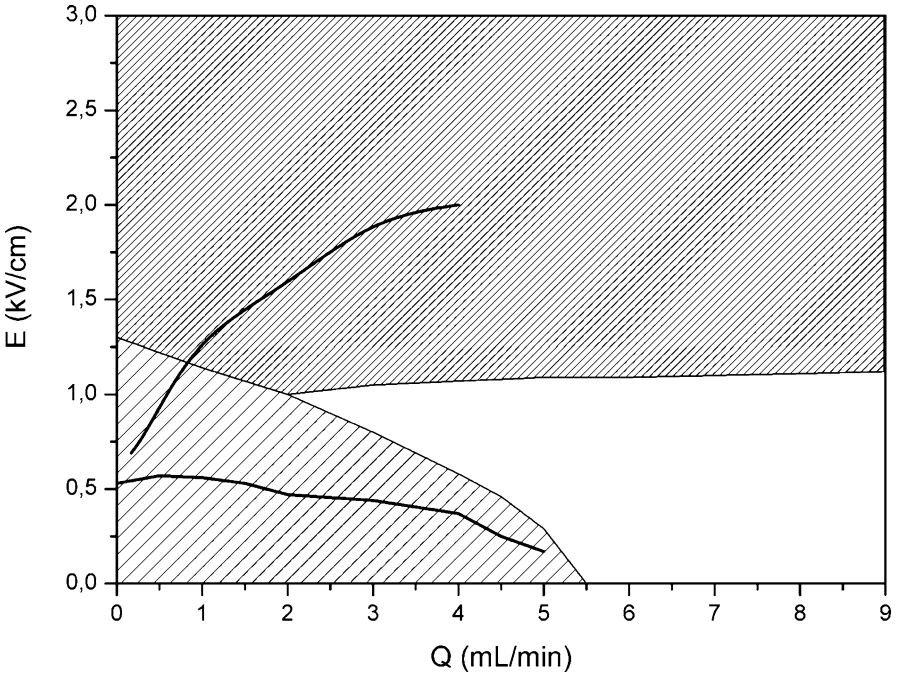

Fig. 9 Example of an operating electric field versus feeding rate diagram for electrospinning adapted from Hohman et al. [32, 33]. The *upper shaded area* shows the theoretically predicted onset of bending instabilities; the *lower* one shows the corresponding onset of axisymmetric instability. The *lines* represent experimental results on the instability thresholds for the two types of instabilities for PEO solutions for a given set of electric conductivity, viscosity, dielectric constant, and surface free energy values corresponding to the ones assumed in the theoretical treatment

trospinning by a suitable choice of field and flow rate on an absolute scale. Further, following the theoretical treatments discussed above, Fridrikh et al. presented a simple analytical model in terms of current and feeding rate, allowing prediction of the terminal jet diameter (beyond which a further thinning due to bending instabilities no longer occurs, as the stresses from surface tension and from surface charge are in balance) [35].

Finally, as far as investigating the electrospinning processes is concerned, it should be pointed out that more phenomena may be observed during electrospinning. One is the occurrence of jet branching characterized by periodic arrangements of the branches extending perpendicular to the jet [13]. Yarin et al. developed a electrohydrodynamic theory which shows that the surface of conducting fluid jets can display complex static undulations at strong electric fields [36]. Such undulations can become unstable for specific conditions leading to the ejection of regular arrangements of lateral branches from the primary jet. It seems feasible that various types of fiber structures may re-

sult such as fluffy columnar networks, called garlands fibers, or even barbed nanofibers as shown in Figs. 1f and 7b.

3
Nanofiber Properties

3.1
Nanofiber Diameters

The diameter of the nanofibers produced by electrospinning is a key parameter for most of the applications envisioned for such fibers. Fiber diameters down to just a few nanometers can be produced by electrospinning from polymer solutions but the diameter can also be extended up to more than 10 μm if required. The most influential spinning parameter to control the fiber diameter is the polymer concentration within the spinning solution. A lower polymer concentration will cause first of all a stronger fiber diameter shrinkage solely by solvent evaporation. Yet, the effect of polymer concentration goes well above this direct contribution, since, in general, polymer concentrations suitable for spinning can be varied only by a factor of well below 10, though fiber diameter variations amounting to a factor of 100 and more are known. A major effect of a variation of the polymer concentration on resulting fiber diameters comes from the corresponding strong variation of the viscosity and the viscoelastic response of the fluid jet to deformations. Both the viscosity and viscoelasticity of polymer solution represented, e.g., by the corresponding relaxation time, are known to strongly depend on the polymer concentration. As far as electrospinning is concerned the variation of these parameters in elongational deformations involving high deformation speeds has to be taken into account. Studies on the capillary thinning process of threads of dilute and semidilute polymer solutions revealed that the deformation happens in two stages the first involving the viscoelastic stretching of polymer coils and the second a quasi-Newtonian flow in which fully stretched coils flow past each other giving rise to a constant elongational viscosity [37]. A further finding which may also be of importance for electrospinning is that such strong and rapid elongational deformation tends to induce chain rupture to a considerable extent.

The dependence of the fiber diameter on the polymer concentration has been investigated for a set of polymers including among others polyamides, polylactides, polyacrylonitrile, polyvinyl acetate or polyethylene oxide [9–13]. One characteristic example is revealed in Fig. 10 for PA 6 dissolved in acetic acid [38].

The diameter changes for polyamide 6 by a factor of more than 10 covering the range from about 150 nm up to about 1.7 μm keeping all other spinning parameters, such as the applied voltage, electrode distances con-

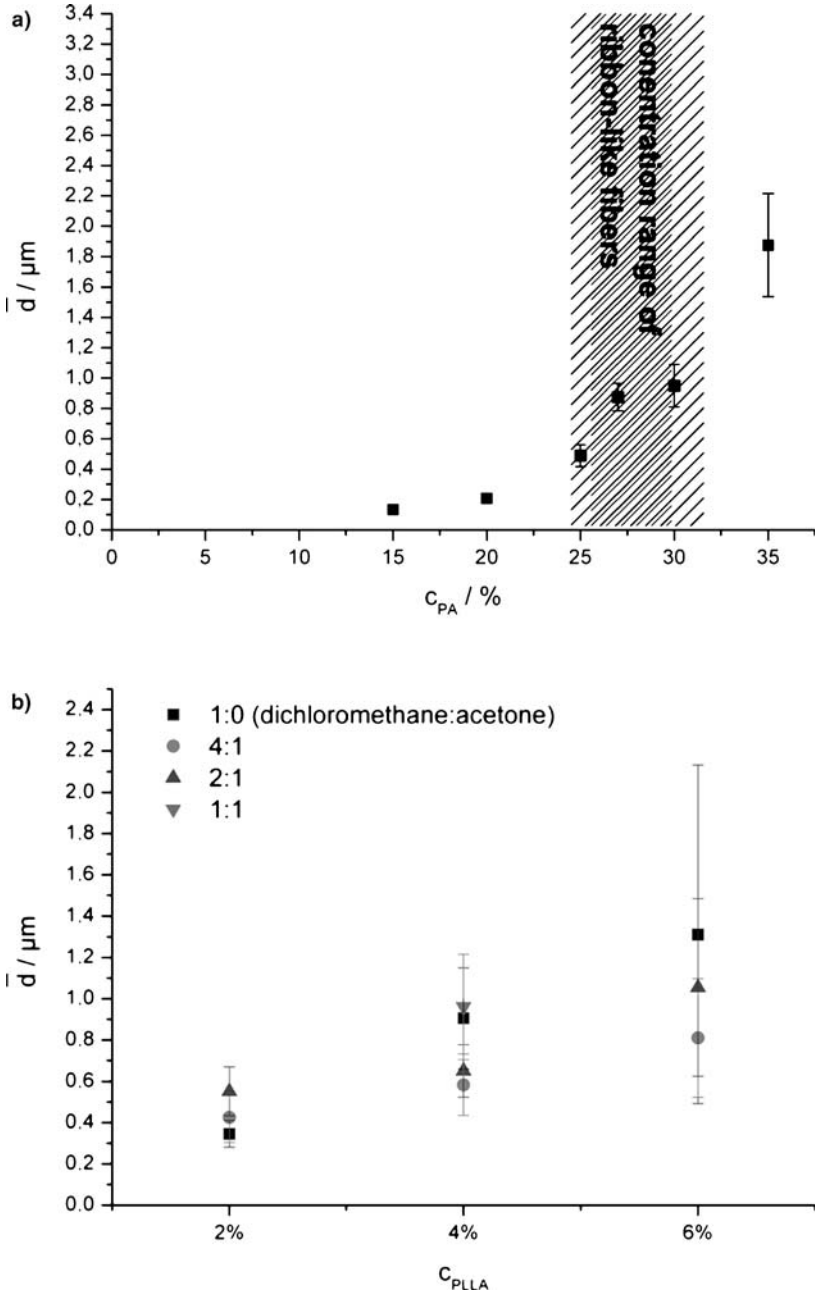

Fig. 10 **a** Dependence of the fiber diameter on the polymer concentration for solution electrospinning [38] for polyamide 6 in acetic acid; in the *shaded area* band-structures rather than fibers with circular cross sections are obtained, **b** Corresponding variation for polylactide in different solvent mixtures

stant, etc. It should be pointed out that one is able to reduce the fiber diameter of polyamide 6 even further to below 50 nm, yet this involves further variations of the spinning parameters beyond the polymer solution concentration. The finding displayed in Fig. 10 a is that the fiber diameter tends to increase in a strongly nonlinear fashion with the polymer concentration, particularly at higher concentrations (similar to the case of corresponding variations of the viscous and viscoelastic properties). The fiber diameters achieved are not strictly constant for a given concentration but rather show a certain distribution which increases in absolute numbers as the diameter increases, yet the relative width of the distribution frequently tends to remain about constant. It is an interesting observation (also indicated in Fig. 10a) that a concentration range exist in which flat band-shaped fibers rather than fibers with spherical cross section are formed. This aspect will be considered below in more detail. Polymer solutions with concentrations below the range showed in Fig. 10 cannot be spun to nanofibers since their tendency to droplet formation is strong at such low concentration unless specific additives modifying the conductivity and other properties are added. On the other hand, solutions with polymer concentrations above the upper values shown in Fig. 10 are, in general, so viscous that again electrospinning fails.

Figure 10b shows corresponding polymer concentration-fiber diameter results for polylactide in dichloromethane. It is obvious that suitable variations of the polymer concentration and of the resulting fiber diameters are much smaller than found for polyamide and that the distribution of the fiber diameters at a given concentration is also broader. These results reflect the different nature of the polylactide solutions in terms of molecular weight, molecular weight distribution, entanglement, interaction with the solvent (which affects both the viscous and viscoelastic properties of the solution). In fact, detailed studies are still sparse trying to relate fiber properties to real data on viscous and viscoelastic properties. A major reason is, of course, that fiber spinning is performed with extremely high strains and strain rates and that, in general, very limited data are available for the viscous/viscoelastic properties for such extreme conditions. Thus, for the time being one has to investigate fiber diameter-polymer solution correlations experimentally for each case of polymer/solvent combinations.

An interesting approach to modify the viscous at viscoelastic properties of a given polymer solution during electrospinning involves the application of ultrasonic agitation to the solution just as it leaves the capillary die [39, 40]. Two effects have been reported. One is that electrospinning of fibers can be extended to higher polymer solution concentration well outside the range accessible without ultrasonic agitation and the other one is that fiber diameter can be modified to a certain extent in this way.

A second spinning parameter which can be exploited to adjust the fiber diameter is the feeding rate, i.e., the amount of polymer solution that is fed per time unit into the spinning apparatus at constant die diameter, and keep-

ing all other spinning parameters constant. Among the examples to be found in the literature are studies on polyacrylonitrile (PAN) which was studied both experimentally and from a theoretical point of view [41]. The result is that again the fiber diameter can be varied in this case by more than a factor of 10 by controlling the feeding rate. Similar results have been reported for other polymer solutions yet it seems that the magnitude of fiber diameter modifications induced via the feeding rate depends strongly on the polymer system under investigations and frequently tends to be rather small.

Polymer concentration and polymer solution feeding rate are not the only spinning parameters that have been evaluated with respect to their impact on fiber diameters in electrospinning. The jet diameters and the fiber diameters can be controlled to a certain extent also by the applied voltage, though again the achieved results vary strongly with the polymer system. It was reported, for instance, for electrospinning of acrylic nanofibers that the jet diameter may decrease initially with increasing voltage, yet that it increased again as the voltage was further increased [42, 43]. This is obviously due to a strong increase of the amount of polymer solution drawn out by the electric field from the capillary. A further approach towards controlling the fiber diameter consists in extending the range of polymer concentrations suitable for spinning to much smaller concentrations and thus smaller polymer fiber diameters by adding components which vary the electric conductivity of the solvent [44]. An increased conductivity tends to increase the charge density at the surface of the jets, thus decreasing the tendency of droplet formation during electrospinning. Finally, a variation of the distance between the spinning die and the counter electrode has been used to affect the fiber diameter. Various effects may contribute to fiber diameter variations, e.g., as the distance is decreased among them an increase in the electric field, a suppression of later stages of elongational processes induced by the bending instability, or the suppression of the complete evaporation of the solvent may have effect. It is for this reason that again the induced fiber diameter variations vary strongly with the polymer system under consideration. Thus, the general conclusion is that as far as solution spinning is concerned the concentration of the polymer solution is the most direct and most general parameter to control fiber diameters in electrospinning.

3.2
Shape of the Fibers

The goal of electrospinning will be in the majority of cases the production of nanofibers uniform in diameter along their complete length and with a spherical cross-sectional shape. In fact, electrospinning tends to produce just such a type of fibers in the range of polymer solution concentrations in which droplet formation is suppressed. This is not really surprising since the geometries of the dies, of the applied field, and, thus, of the deformation of

the droplets are in the majority of cases axially symmetric. Furthermore, the fibers tend to be straight for a significant persistence length often larger than 10 cm and above. This becomes particularly evident if the fibers are deposited in a parallel fashion due to particular electrode configurations to be discussed below in more detail. Yet, in several cases fiber shapes have been reported showing strong buckling (Fig. 11) [19]. Buckling obviously results from the presence of longitudinal compressive forces acting on the impinging thread. Detailed investigations of the buckling phenomenon have revealed a surprising richness of buckling pattern including sinusoidal trajectories, meandering, coiled structures, figure eight structures double pattern, and many more. Further, the trajectories of the deposited nanofibers may result from a superposition of the looping motions due to bending instabilities and buckling.

Nanofibers with spherical cross sections are the general target for the majority of applications introduced previously. Yet, considering the prism-shaped silk fibers and the corresponding peculiar optical properties, other types of fiber cross sections may be beneficial for specific applications. In fact, electrospinning yields, either by poor controlling or on purpose by an appropriate controlling, a variety of fiber cross-sectional shapes originating from the complex self-assembly processes intrinsic in electrospinning.

One frequent observation is the formation of band-shaped fibers characterized by a flat rectangular cross-sectional area [45]. An example of such a fiber shape is shown in Fig. 1b. It results, for instance, in a very limited range of polymer concentrations in the case of polyamide 6 spun from acetic acid solutions, while fibers with spherical cross-sectional shape are formed outside this concentration range. Band-shaped fibers have also been reported for polymers such as polycarbonate and many more.

A tentative explanation for the formation of such band-shaped fibers in electrospinning is that the solvent evaporates particularly rapidly in many in-

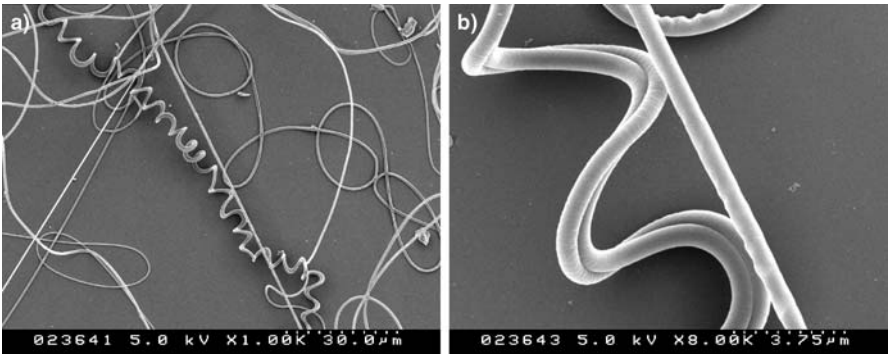

Fig. 11 Buckling PA 6 nanofibers electrospun from formic acid solutions. (Fibers shown for different magnifications)

stances from the surface of the fluid jet giving rise to a solid surface shell [45]. The subsequent evaporation of the remaining solvent in the core area gives rise to hollow fibers. These in turn are assumed to collapse in such a way that band-shaped fibers result. In fact there are indications based on optical studies that such a process actually takes place in certain cases. Yet, the observation for polyamide 6 systems that the formation of band-shaped fibers is restricted to a very narrow concentration interval with fibers displaying a spherical cross section forming on both sides of this concentration interval suggests that this may not be the only mechanism yielding such special fiber shapes [38]. In any case such fiber cross-sectional shapes can be prepared reproducibly and they could well be of interest for specific applications. Nonwovens composed of them should display total porosities, pore sizes, and permeation properties differing significantly from those composed of fibers with spherical cross-sectional areas.

Fibers characterized by droplets or spindle type elements arranged along the fiber in a regular or random fashion is a further frequently observed nanofiber structure in electrospinning. Figures 1d and 12a give examples of such structures. The origin of such structures seems to be that the bending instability tending to produce nanofibers with uniform diameter becomes superimposed by other instabilities notably the axisymmetric instability as suggested by the theoretical operating diagram discussed previously. Spinning nanofibers from dilute solutions, from solutions in which the electric conductivity is below a critical value, and also spinning polymers for which the molecular weight is too small (meaning no chain entanglements are formed) are reasons for such fiber structures. These are in the majority of cases unwanted and can be suppressed by a suitable variation of the processing parameters. Adding specific low molar mass compounds to enhance the ionic conductivity is one possible approach that has been demonstrated for various polymer systems [44]. On the other hand in special cases like drug delivery such structures may be beneficial and can thus be produced reproducibly.

Another feature of interest is fragmentation of electrospun nanofibers to linear segments or droplets. In general the integrity of the nanofibers is a major requirement for many of the applications introduced above among them textiles, filter applications and in particular also nanofiber reinforcement. This integrity should survive processing steps involving heat treatment occurring during filter formation or textile production, or during the incorporation of the fibers into a polymer matrix to be reinforced. Furthermore, applications may also require the nanofibers to be stable at enhanced temperatures for longer time intervals. Nanofiber modified surfaces displaying ultrahydrophobic properties [46] might also be subjected to further coating steps involving again enhanced temperatures. The integrity of the fibers is a requirement in all cases, i.e., fragmentation processes should be absent.

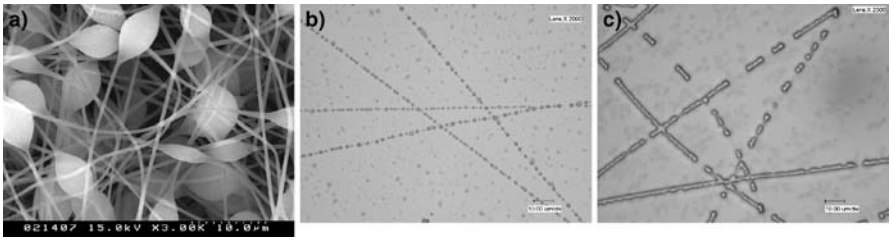

Fig. 12 **a** Beaded fibers (PS), **b** PA 6 nanofibers decomposing into droplets via Rayleigh instabilities. **c** Polystyrene nanofibers decomposing to linear segments as intermediate states of fragmentation [89]

In other cases fragmentation might be something which is wanted. A complete or partial fragmentation of nanofibers to nanodroplets may be of interest for further modification of surface properties of substrates involving superhydrophobicity [46]. To induce such structures in a highly controlled way one may also start from solid nanofibers and anneal them at elevated temperatures where the polymers become soft. Conventional Rayleigh instabilities controlled by the surface energy can thus be induced, which cause the formation of a pearl necklace structure with a uniform size and spacing of the droplets along the fiber, as obvious from Fig. 12b [47, 48, 89]. The diameter of the droplets and their distance is controlled to a major extent in this case by the original fiber diameter. As intermediate state, a fragmentation into linear segments that can be conserved by cooling may appear as shown in Fig. 12c. Self-organization may thus be used to produce nanowires from nanofibers.

Finally, complex fiber structure with branchings, spikes extending from the fiber backbone, have been observed (see examples in Figs. 1f and 7b). Up to now no explanations exist for their formation other than that they may be the consequence of a further pathway following self-organization controlled by Coulomb interactions possibly involving splaying at its early stage. Again such structures can be produced in a reproducible manner and may find specific applications in the future.

3.3
Nanofiber Topologies, Porous Fibers

Electrospinning generally yields fibers with smooth surfaces, as shown in the discussions above, if the key electrospinning parameters are controlled in such a way that the self-assembly processes are directed along this line. Yet, keeping these spinning parameters constant but choosing the spinning solution appropriate to other types of self-assembly effects can be superimposed. Phase separation between solvents and polymer species both for the case of a single solvent or solvent mixtures, phase separation effects between polymers in spinning solutions composed of more than one polymer, between

a polymer and low molar mass additives, and condensation effects of water vapor initiated on the surface of the jet can be exploited in a controlled way to give rise not only to specific supermolecular structures but also to specific surface topologies.

It is well known from thermodynamics of mixtures that phase separations may take place leading to two types of phase structures depending on the concentration ranges considered, the molecular interactions between the components, the temperature, on the time scale in which separation takes place and also on the mechanical stresses present. It is rather difficult to make quantitative predictions for the electrospinning process even if the phase diagrams are known for the solutions under study. Qualitatively two types of phase morphologies, the bimodal or the spinodal type, should occur if phase separation takes place during electrospinning respectively [49]. Phase separated domains dispersed within a continuous matrix are characteristic for the bimodal case and a co-continuous phase morphology with a certain regularity of the arrangements of the different phases for the spinodal case. In electrospinning of fibers the final phase morphology found in the fibers and the composition of the phase are modified by the evaporation of the solvent and the strong elongational deformation.

One direction which has been investigated along this line is preparation of porous fibers with various types of pore sizes, pore arrangements as well as with various magnitudes of the total porosity and thus of specific surface areas. These are of interest for a variety of applications, e.g., tissue engineering, filter technique, catalysis, drug delivery, nanofiber reinforcement, and many others. Pores can function as anchorage for cells in tissue engineering. They may increase the surface in filter applications or catalysis by up to one order of magnitude, may modify wetting properties and thus matrix fiber coupling in the case of fiber reinforcement, and can be exploited to modify the release kinetics of drugs. Pores can also influence the kinetics of biodegradation of biodegradable nanofibers.

The most direct way to produce porous fibers consists in spinning the fibers still containing solvents on very cold surfaces or directly into liquid nitrogen causing in both cases an instant phase separation into solvent and solid polymer [50]. Freeze-drying approaches can then be used to remove the solvents from within the solid polymer fibers yielding highly porous polymers. This was shown for polystyrene, polyacrylonitrile, polycaprolactone, as well as polyvinylidenfluoride. One disadvantage of this approach is that one needs a subsequent treatment of the fibers (freeze drying) and a transfer of the fibers to the target substrate

A second and somewhat more direct approach is based on water vapor condensation processes in humid environments [51, 52]. The model consideration is that the spinning jet is cooled down due to solvent evaporation and that the tiniest droplets of water consequently precipitate onto the spinning jet. These droplets then form the pores in the solidified fibers. The extent of

pore formation and also pore sizes can be tuned by variation of humidity. The pores which result tend to assemble predominantly on the surface of the fibers and to display a spherical shape. It thus seems that they frequently do not experience longitudinal deformations taking place in electrospinning to an appreciable extent.

Another approach towards porous structures relies on phase separation into polymer rich and polymer depleted regions as evaporation of the solvent takes place (this can generally be roughly estimated from phase diagrams), yielding polymer rich regions and polymer depleted regions that will form pores in the solid phase if the solvent is completely evaporated [53]. The extent of the pore formation is thereby defined by the relative percentages of both phases. Employment of solvent mixtures allows a selective adjustment of porosities. Figure 1c illustrates examples of porous polylactide nanofibers that were fabricated by this method. It is apparent that the degree of porosity can be varied strongly and that the pores may be elongated.

Entirely different fiber topologies are obtained if nanofibers are spun from a solution of mixtures of immiscible polymers in the same solvent [53]. Phase separation occurs with the evaporation of the solvent, leading to binodal or spinodal structures, respectively, in the nanofibers depending on the system. To generate porous fibers of high overall porosity two strategies are possible [54]:

1. Highly swelling solvents induce significant increases in fiber diameter and a highly porous structure (Fig. 13) with porosities of 75% and more remains after removal of the swelling agent.
2. Removal of one of the phases in the case of the previously mentioned binodal or spinodal segregation by specific solvents yields highly porous

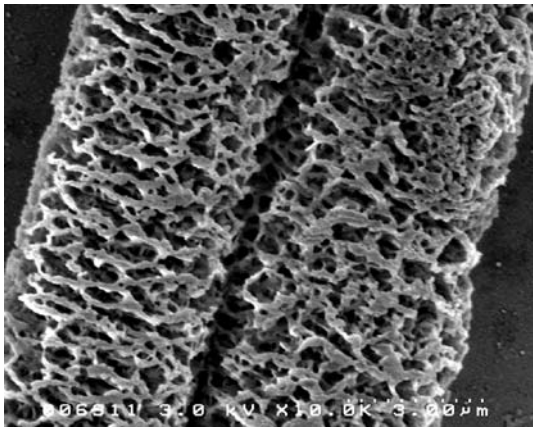

Fig. 13 Porous nanofibers obtained via phase separation processes during electrospinning for mixtures of polylactide and polyethylene oxide [54]

fibers even with periodic arrangements if a spinodal phase separation between the two polymers under consideration has taken place.

Approaches based on phase separation of polymer components and the selective removal of one of the components may also be directed in such a way that fibers without pores yet characterized by fractal surfaces (Fig. 1e) result. Such types of fibers can be predominantly obtained for specific concentration ranges of the two polymers and for spinodal decompositions.

3.4 Internal Morphology

The internal structure of electrospun nanofibers will be controlled in principle by three major contributions:

1. Glass formation and crystallization as in the bulk, governed by thermodynamic and kinetic factors;
2. Rapid mechanical deformation characteristic of the jet deformation in electrospinning;
3. Confinement effects arising from the small scale of the resulting fiber diameters.

In the majority of cases nanofibers are produced by electrospinning from solutions. Fiber formation is controlled by the simultaneously proceeding processes of solvent evaporation and strong elongation of the solidifying fibers. A volume element of the jet travels the whole way from the spinning die to the final deposition of the solid fiber on the counter electrode in a time frame of typically 10^{-1} s. The time span for the structure formation within the resulting nanofibers is therefore typically 10^{-2} s and below. In this respect, electrospinning resembles spincoating in which nanofilms are cast from solution by transferring droplets of the solution onto a rapidly rotating substrate. Freezing-in of amorphous regions into a glassy state, a partial crystallization incorporating the formation of lamellas, the formation of orientational orders for the chain molecules and the crystals, and the formation of supermolecular structures (such as spherulitic structures or phase domains as far as blends are concerned) (see above) are processes happening in both electrospinning and spincoating within the solidifying fibers or films during a very short time scale. One major topic to be discussed in the following is the effect of the short time scale on the structure formation and on the properties of the resulting structures. The second major topic is the effect of the confinement imposed by the small diameter of the fibers on structure formation and properties. It is well known that confinement affects structure formations, molecular dynamics and properties [55]. In the following the discussion will distinguish between polymers unable to crystallize, e.g., atactic polystyrene, atactic polymethylmethacrylate, and those that can, e.g., polyamides, polylactides, polyethylene oxide and many more.

3.4.1 Amorphous Polymers

A polymer that is unable to crystallize will experience a freezing-in process in a specific temperature range, which depends on the individual polymer that is being considered [56]. The freezing-in process does not correspond to a thermodynamic phase transition but is rather a kinetic transition from the supercooled molten state (a thermodynamically equilibrium state) to the nonequilibrium state of a frozen melt. This transition is accompanied by a rapid increase in relaxations times, viscosities, mechanical moduli. A characteristic feature of the glass transition is that the location of the transition temperature depends on the thermal history. It increases as the speed with which the cooling process proceeds is increased. Yet, despite the rapid fiber formation and solidification process characteristic of electrospinning no significant deviation of the glass transition temperature of nanofibers from the one of the bulk material has been reported so far.

The glass transition temperature has furthermore been claimed to depend strongly on confinement effects. A decrease of the glass transition temperature of several 10 K has been claimed for nanofilms as the film thickness approaches values of 10 nm and below. Yet, it seems that such strong shift can frequently be accounted for by degradation processes taking place during preparation and annealing of such thin films at elevated temperatures and that nanofilms prepared in vacuum or in nitrogen atmosphere do neither show degradation nor a significant depression of the glass transition temperature even for films with thicknesses in the 10 nm range [57, 58]. It is therefore not surprising that no depression of the glass transition temperature of nanofibers relative to the value of the bulk material has been reported so far.

A further feature of the freezing-in process is that not only the glass transition temperature but also properties within the glassy state, i.e., density, enthalpy, moduli, etc., depend on the speed with which the glassy state is approached [56]: the properties of the glassy polymers in nanofibers might strongly differ from those of fibers formed more slowly. One feature which can be looked upon as a manifestation of the particular state of the glass is the physical aging process. The nonequilibrium glassy state tends to relax towards the equilibrium state of the supercooled melt and this relaxation depends on the speed with which the glass was formed. Enthalpy relaxations related to aging and volume relaxations, again related to aging, can be analyzed by calorimetry and dilatometry respectively. Calorimetric studies reveal the glass transition in the absence of aging processes by a stepwise increase of the specific heat at the glass transition temperature on heating due to the onset of additional degrees of freedom. Aging processes of the enthalpy manifest themselves by the superposition of this stepwise increase by additional maxima or minima in the heat flow. There are only few statements concerning this phenomenon in electrospun nanofibers in the literature [59]. Electrospun

nanofibers of semi-crystalline polylactide nanofibers show distinct deviation of the heat flow from the usual step-like increase for the amorphous regions, indicating aging processes

The induction of chain orientation via electrospinning in glassy polymers is a topic of considerable interest in basic research but also with respect to applications. The experimental analysis of electrospinning processes shows, as discussed above, that the elongation of the fibers is very high, up to a factor of 10^5, while the elongation rates simultaneously reach values of $10^5\ s^{-1}$. Estimations are made according to which chains become highly oriented, as in the case of when the product of the elongation rate and chain relaxation time is higher that 0.5 [25]. For polymer solutions suitable for electrospinning, the appropriate ranges of their molecular weights and polymer concentration relaxation times of 10^{-3} to 10^{-2} s were reported [13, 19, 37]. A significant chain orientation should thus be generated during electrospinning. It is still an unanswered question whether the deposited fibers continue to contain traces of solvent that would promote chain relaxation. This should depend on the vapor pressure of the solvent, amongst other parameters.

As a matter of fact the results of experimental studies on the occurrence of birefringence are rather inconsistent. In some cases a slight birefringence was observed, e.g., in polybenzimidazol nanofibers with diameters around 300 nm, as well as in nanofibers from styrene-butadiene-styrene triblock copolymers with diameters of about 100 nm, as shown by Kim et al. [60]. The latter systems, of course, already contain some kind of order. In other cases nanofibers that did not show birefringence and therefore obviously feature no chain orientation were obtained from purely amorphous polymers, such as polystyrene and others. It is not entirely understandable why amorphous nanofibers do not generally show high chain orientations in view of the deformation rates typical for electrospinning and of the relaxation times characteristic for the spinning solutions. There still quite clearly remains a need for systematic investigations. In any case it has to be anticipated that nanofibers displaying orientations will shrink if heated to higher temperatures or come into contact with solvents which cause swelling.

3.4.2 Partial Crystalline Nanofibers

An opinion which is frequently voiced as far as nanofibers formation by electrospinning is concerned is that the structure in nanofibers and the properties of the growing crystals should deviate strongly from the one of bulk systems due to rapid structure formation and confinement effects imposed by the small diameter of the fibers. Melting point depressions originating from a reduction in size of the crystals are well known from metals or semi-conductor systems. Yet, no such effects actually seem to be of general significance in electrospun polymer nanofibers. One has to take into account in this con-

text that the crystallization in polymers, resulting crystal sizes and crystal shapes differ in many aspects from the one taking place in low molar mass materials [61].

One feature is that polymers tend to crystallize only to a certain extent characterized by a degree of crystallinity, which may amount to significantly less than 50%. The depression of crystallization originates primarily from the strong entanglements of the polymer chains in the melt or in highly concentrated solutions. These restrict configurational changes necessary for crystallization. A further feature is that polymers tend to form lamellar crystals with lamellar thicknesses in the few nanometer to 10 nm range already in the absence of confinement. The lamellar thickness and thus the melting temperature of the lamellae depend predominantly on the thermal history for kinetic reasons. Finally, the crystal structures usually contain defects, e.g., coming from chain ends. These features suggest the possibility that solidification of nanofibers comprising crystallization will not be too different from the one taking place in the bulk, which turns out to be true.

In fact, there are no explicit indications in the literature that solidification processes in electrospun nanofibers related to crystallization are significantly different from those in bulk. It was, for instance, reported for the case of nanofibers from PET, polyethylenenaphthalate, and mixtures of these polymers that the melting points are not modified to an appreciable extent by the processing of the polymers into nanofibers. At the same time, it was reported that the degree of crystallinity may be increased as well as the glass transition temperature and the crystallization temperature [62]. The authors, however, indicated that transesterification processes occurred in the polymer mixtures and that, therefore, a decrease of chain lengths of chain molecules during electrospinning has to be anticipated. In the case of polylactide, it was observed that the degree of crystallinity as well as the melting point of the electrospun fibers were very similar to those of macroscopically prepared samples [63].

There are several studies concerning electrospinning of polyamides. It was reported that electrospinning of PA6 yields nanofibers that form the less ordered γ-crystal modification as obvious from X-ray diffraction and Raman investigations [64, 65]. Crystallization from bulk solution resulted in the ordered α-form. In this regard it is interesting that in the case of conventional fibers fabricated by melt extrusion the formation of crystals proceeds similar to the one of the crystal formation during electrospinning, despite all differences in the fabrication of the fibers. This holds especially when the elongation after extrusion exceeds a definite limit. In this case the less ordered γ-phase is observed. Therefore, the reasoning is that the development of the γ-form in nanofibers is a distinct indication of strong mechanical deformations occurring during electrospinning. This phase can be converted into the higher ordered α-phase by annealing of the nanofibers at higher temperatures.

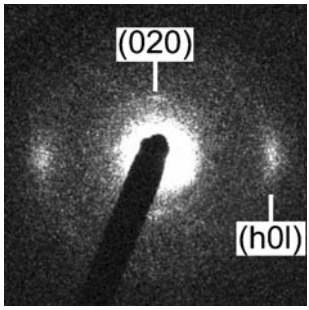

Fig. 14 Selected area electron diffraction diagram (SAED) obtained for a single PA 6 nanofiber [63, 65]

Of particular significance for mechanical properties of the fibers is the chain orientation and the orientation of the crystallites, which show up in the electrospun fibers as again made obvious from Raman investigations, X-ray or electron diffraction studies, and other indicators. Very high crystallite orientations in nanofibers from poly(ferrocenyldimethylsilan) were shown by Chen et al. who pointed out that the perfection of orientation could be substantially increased by annealing the fibers [66]. This orientational order is particularly striking if diffraction experiments are carried out on single fibers. Applying the so called SAED (selected area electron diffraction) technique the degree of orientation of the crystals in a PA6 nanofiber with a thickness of 50 nm was analyzed [63]. These diffraction experiments revealed the presence of very high crystallite orientations in the individual nanofibers produced by electrospinning (Fig. 14). This is apparent from the inhomogeneous azimuthal distribution of the diffraction intensity. Comparable orientations can only be achieved in macroscopic fibers produced by melt extrusion if the extrusion is followed by extreme deformations.

For the particular case of nanofibers made from liquid crystalline polymers, using a polyhexylisocyanate as example, it was demonstrated that the degree of orientation can depend greatly on the fiber thickness. Jaeger et al. furthermore report that in PEO fibers especially surface layers may be highly oriented [67]. Finally, polymer nanofibers composed of a single nematic monodomain were observed for main chain liquid crystalline elastomers, which were cross-linked during electrospinning via UV-light irradiation [68].

3.5 Mechanical Properties of Single Nanofibers

Single nanofibers produced by electrospinning can be expected to display quite unusual mechanical properties. The intrinsic structure of nanofibers as controlled by the freezing-in, crystallization, and elongational processes was already discussed above. Strong orientations of both chain molecules and

crystals are known to affect mechanical properties such as the tensile stiffness and tensile strength considerably [69]. One reason is that these mechanical properties become more and more controlled by deformations of the covalent chemical bonds – i.e., their length and the angle between the bonds along the chain backbone – rather than by the corresponding deformations of van der Waals bonds acting between the chain molecules. A second reason is that the strong deformations of the polymers during electrospinning may give rise to modified crystal modifications, perhaps showing enhanced mechanical properties. Finally, it is known from other materials that a reduction in fiber diameter tends to enhance the strength of fibers as demonstrated by the so-called Griffin criterium [70].

Experimental investigation on the stress strain behavior of single electrospun nanofibers can only scarcely be found in literature so far, the analysis being mostly carried out via AFM methods. These studies very explicitly show that electrospun nanofibers possess very good mechanical properties. For example, moduli of up to 50 GPa and above were reported for polyacrylonitrile fibers [71]. The fibers showed high orientations according to X-ray analysis. Bulk samples of PAN without orientational order display moduli of only 1.2 GPa; the increase of the modulus by electrospinning is therefore quite significant. For polyethylene oxide nanofibers moduli were observed that were distinctly higher than the ones of bulk samples [72]. In this case again the orientation induced by electrospinning is the principal reason. In contrast to these results moduli of only 0.9 GPa were observed for nanofibers based on polyvinylpyrrolidone and containing titanium dioxide nanoparticles [73]. However, there are no statements on the orientational state in this case. It is in any case obvious that nanofibers feature very high moduli if the crystallite and chain orientation is high. Such fibers are thus of great interest among others for the application in nanofiber reinforcement.

4
Nonwovens Composed of Electrospun Nanofibers

Standard electrospinning devices such as the single or multiple syringe type die arrangements arranged opposite to a flat extended counter electrode (see Fig. 2 as an example) will give rise to so-called nonwovens displayed in Fig. 5. As far as the deposition of infinitely long fibers is concerned, fibers or segments of the fibers are deposited continuously within a certain area of the counter electrode or substrates on top of it. The layer thickness is controlled via the thickness of the fibers and the total coverage as specified, for instance, by the total weight of fibers per unit area. The planar extension of the nonwoven is controlled on the one hand by the bending instability giving rise to extended loops (see above) for a given electric field and on the other hand by the distance between the two electrodes. Taking a distance of 15 cm as an ex-

ample the diameter of the deposited nonwovens tends to amount to 10–25 cm for a single syringe type die.

Such nonwovens also arise from electrospinning setups in which the feeding electrode consists of a wire or cylinders with spikes attached to them, again using a nonstructured counter electrode. A specific feature of such nonwovens that is already obvious from Fig. 5 and that will be discussed below in more detail is that it is highly porous. In fact, the total porosity, i.e., the volume taken by the pores relative to the one of the total nonwoven, may amount to 90–95%. The pore sizes are subjected to a significant distribution to be discussed below and the average pore dimensions tend to be different in the plane of deposition and perpendicular to it. Such nonwovens are of interest for filter and textile applications as well as for tissue engineering the filter efficiency, thermal insulation, or the growth of stem cells depending strongly on details of the pore structures. Furthermore, thin layers of such nonwoven may serve as surface coating, e.g., for modification of the wetting properties of the substrate all the way towards self-cleaning in analogy to the lotus effect.

4.1 Fiber Arrangement in Nonwovens

Electrospinning performed with planar counter electrodes, substrates located on them, and also moving substrates such as filter paper or textiles will give rise to a random planar deposition of the nanofibers (Fig. 5). Nonwovens thus result with an isotropic fiber orientation within the plane of the nonwovens and a layer-like arrangement of such nanofibers in the third dimension specifying the thickness. Yet, electrospinning is really not limited to the production of such nonwovens with a statistical planar orientation. The orientation of nanofibers along a certain direction is of interest for nanofiber reinforcement or for tissue engineering in order to allow a distinct growth direction for the cells and for many more applications to be discussed later.

Parallel fibers can, for example, be obtained using rapidly rotating cylindrical collectors which either serve as counter electrode or are combined with further electrode arrangements [64]. The collectors usually have the shape of long rotational cylinders but can also be wheel-shaped. Furthermore, parallel fibers can be realized by special electrode arrangements consisting of two flat plates aligned parallel to each other or corresponding frame-shaped electrodes, respectively [62, 74]. The degree of orientation of the fibers can be increased quite significantly by this method (Fig. 15). Another possible modification of the electrodes is a quadratic arrangement of four electrodes that leads to a cross-shaped deposition of nanofibers [75]. Further variations along this directions suggest themselves.

High degrees of orientations were achieved also by a distinct decrease of the distance between the electrodes down into the mm or even μm range in combination, for instance, with a finely tip-shaped spinning electrode or

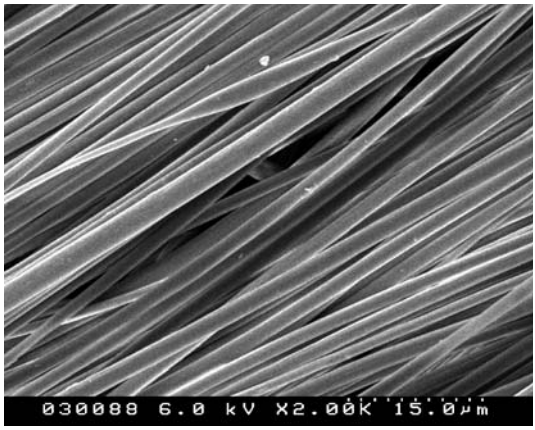

Fig. 15 Parallel PA 6,6 fibers obtained via electrospinning on rotating type electrodes

counter electrode respectively [76–78]. To obtain three-dimensionally oriented fiber arrangements within the nonwovens the needle punching technique known from conventional nonwovens made of macroscopic fibers or the solidifications using water jet treatment are possible means. Yet, there is no reference in literature referring to this technique as far as nonwovens made of nanofibers are concerned. Finally, it has to be pointed out that strong interest currently exists towards the formation of textile fibers via electrospinning.

4.2 Heterogeneous Nonwovens

It is generally the aim to prepare nonwovens with fibers of uniform thickness and from material of a particular chemical composition throughout the nonwoven. The reason is that in such case both the pore structure and the nature of the surfaces are uniform which allows better predictions for pore structure and adsorption properties (see below) and which may be of benefit for specific applications

Yet, it is also beneficial to a variety of applications to construct nonwovens with fibers of non-uniform thickness to, for example, introduce pore size gradients or modify transport properties. Experimental studies already discussed above and also theoretical treatments show that by proper choices of solvent and concentration of the spinning solution the fiber diameter for one and the same material can be varied by a factor well above 10. Good examples are polyamide or polyacrylonitrile, respectively. A possible approach towards nonwovens composed of nanofibers with different yet specified diameters consists in using a multi-jet electrospinning setup as represented by a parallel arrangement of several syringe type dies close to each other. Spinning solutions containing different concentrations of the same polymer, which are

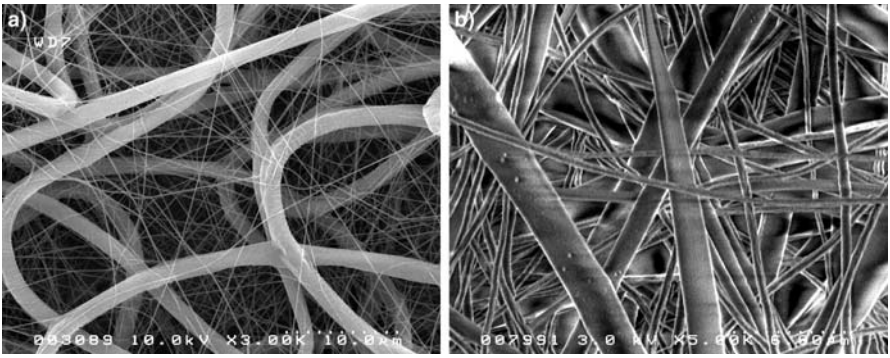

Fig. 16 Nonwoven composed of: **a** Thick nanofibers and thin PA 6 nanofiber, **b** Thick polyamide 6 (PA 6), and thin polylactide fibers [38]

fed through these dies, will give rise to nonwovens with nonuniform fiber diameters [38]. Two examples are given in Fig. 16, showing that the ratio of the fiber diameters within one nonwoven can be well above a factor of 10. Furthermore, by selecting the composition of the spinning solutions appropriately, one is even able to construct the nonwoven from fibers with spherical and flat cross-sectional shapes. This way, one becomes able to modify pore structures and adsorption properties correspondingly.

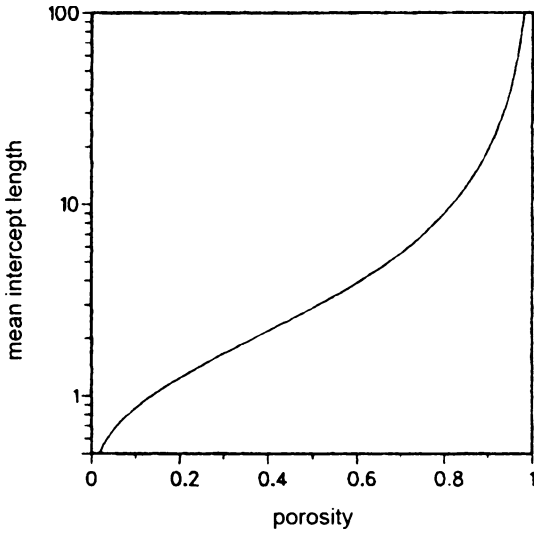

Fig. 17 Relation between reduced pore size (pore size relative to the fiber diameter) mean intercept length), and total porosity for arrangements of unimodal nanofibers, adapted from [81–83] as obtained from Monte Carlo simulations

Along the same line chemically inhomogeneous nonwovens can be produced with multi-jet arrangements accordingly by pumping polymer solutions composed of chemically different polymers through the dies, an example for a nonwoven is displayed in Fig. 16b. It is composed in this case of polyamide and polylactide nanofibers. In addition one can, of course, also control the fiber diameters of the two polymers with respect to each other, adding a further degree of inhomogeneity to the nonwoven.

Such chemically inhomogeneous nonwovens are of interest for specific applications. For tissue engineering, for example, heterogeneous carrier matrices based upon micro- and nanofibers, e.g., from PEO, collagen and segmented polyurethane, were fabricated by either sequential or simultaneous electrospinning [79]. A cylindrically shaped structured tissue based on thin collagen nanofibers as inner layer and thick polyurethane fibers as outer layer was found to constitute a good carrier matrix for artificial blood vessels.

4.3 Porosity and Pore Structures

The pore structures characteristic for these kind of fiber-based nonwovens determine the gas diffusion through the fibers, the resistance towards airflow, filter effectiveness, and the suitability as carrier for tissue engineering, e.g., for stem cells. So far only a limited number of experimental results on pore dimensions and internal surface areas were obtained. Scanning electron microscopical observations such as the ones displayed in Figs. 5 and 16 indicate that the pores are not spherical but rather anisometric assuming odd shapes as given by the multitude of linear fiber segments crossing each other, thus defining the surface of the individual pore. The average pore diameters are broadly distributed and are for fiber diameters of some 100 nm in a range between some 10^3 and 10^4 nm. However, these values can be distinctly modified by the control of the overall porosity defined as the volume taken by the pores relative to the total volume of the nonwoven. This parameter can, for instance, be determined from the total volume of a piece of nonwoven and its mass taking the density of the nanofiber material into account. More detailed information becomes available by using various types of porosimeters, e.g., mercury-porosimetry or nitrogen porosimetry detailing the total pore volume, average pore sizes, as well as the magnitude of the total specific surface area [80]. Such studies are currently extremely limited for nanofiber nonwovens.

In fact, the analysis of details of the pore structures of nonwovens particularly composed of nanofibers is not an easy task particularly if one is interested in their dependence on the orientational distribution of the fibers within the nonwovens. Planar isotropic arrangements, arrangements of parallel fibers in a given plane or fiber arrangements characterized by a three-dimensionally isotropic arrangement should result in different pore structures and corresponding permeation properties. It is of interest to learn how

pore sizes are controlled by fiber diameters and perhaps at given diameters by the specific mechanical properties of the fibers, whether they be stiff or flexible.

Theoretical studies both analytical ones and simulations often dating back several decades have already proven themselves to be extremely helpful in this matter. In fact, such studies were motivated in the context of classical nonwovens composed of fibers with diameters well in the 10 micrometer range aiming at applications in filters or textiles. The predictions of such theoretical studies were displayed in reduced quantities, scaling with the fiber diameters so that the predictions can also be, to a certain extent, directly adapted to nonwoven prepared from nanofibers. One has to keep in mind, however, that the flow pattern may change significantly as the fiber diameter approaches the few nanometer scale as controlled by corresponding Knudsen numbers. The Monte Carlo approach taken for predicting nonwoven properties is particularly transparent since it mimics the deposition process taking place in electrospinning closely [81–83]. It will be used therefore in the following for the discussion of the pore structure of nonwovens.

In these Monte Carlo simulations linear fiber segments with a given fiber diameter are deposited on a model plane one after the other. Their individual orientations are chosen by various methods in such a way that either planar isotropic, planar parallel, or even three-dimensionally isotropic fiber orientations are mimicked. Furthermore, the fiber coverage per unit area can be specified, thus yielding nonwovens of different total porosity. The next step concerns the analysis of the pore structures. To this end quantities such as the mean intercept length can be calculated from the simulated structures. An intercept length typically represents the length of a linear segment oriented in a given way, which just fits into a pore bordered by the nanofibers. Within the framework of this paper the intercept length is given relative to the fiber diameter. The average is then taken with respect to all segment orientations and all positions in the nonwoven. Such a quantity can be taken as a good representation of the average linear dimension of a pore. Figure 17 displays a general correlation between the reduced fiber diameter and the reduced intercept length as a function of the total porosity.

One obvious result is that the higher the porosity the bigger the average pore size in nonwovens for fibers of constant radius. Values of the specific surface of nanofibers are typically in the range of 500 m^2/g and 10 m^2/g for nanofibers in the range of 10 to 500 nm. One rather surprising prediction is that as far as diffusion and permeation properties are concerned the orientational order of the fibers in nonwovens does not really play a significant role for larger total porosities as characteristic for electrospun nonwovens. Strong differences occur at small total porosities in agreement with the predictions of corresponding analytical treatments.

Monte Carlo simulations show furthermore that the overall porosities of nonwovens are significantly decreased with increasing flexibility of the

fibers [84] (Fig. 6a) and that a chemical vapor deposition (CVD) [85] which leads to the construction of a shell around the fibers can distinctly decrease the porosity as well [86]. The simulations have been extended to predict the diffusional properties of gases in such nonwovens, the pressure drop in air filtration, the filter efficiency in aerosol filtrations, the permeation of viscous fluids, etc. [81–83, 87]

4.4
Mechanical Properties of Nonwovens

The mechanical properties of the nonwoven are of interest if, for example, they are used as template for seeding stem cells in tissue engineering. The mechanical properties should be similar in this case to the ones of the tissue to be replaced. Tissues such as cartilage tissue for example or also skin tissue are typically characterized by elongation moduli (stiffness) ranging between some 10 to some 100 MPa, by maximum deformation stresses (strength) of some 10 MPa and maximum deformations of about 10 to 200%. To obtain corresponding data for nonwovens made of nanofibers these nonwovens are subjected to stress-strain investigations, for instance, with commercially available mechanical testers. For electrospun nanofibers which do not show a specific molecular orientation along the fiber axis and which are based on soft elastomers values for the modulus of about 3 MPa, for the maximum stress of about 9.6 MPa and for the maximum elongation of about 360% are reported [88]. In contrast nonwovens made of significantly stiffer polyamide fibers (Fig. 18) display

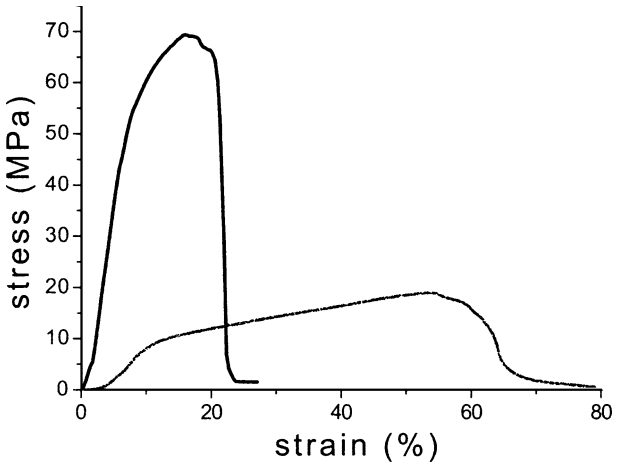

Fig. 18 Stress-strain experiments performed on polyamide 6/6T nanofiber nonwovens [89] with the fibers either parallel (*blue*, *upper curve*) or perpendicular (*red*, *lower curve*) to the deformation direction

values for the modulus of about 100 MPa, the tensile strength amounting to 20 MPa and the maximum elongation to 53% [89]. It is furthermore evident that nonwovens in which the fibers are oriented along a preferred direction within a plane should exhibit enhanced mechanical properties. In fact, the modulus increases due to fiber orientation from 100 to 900 MPa for PA 6 fibers oriented along the elongation direction. The tensile strength is increased from 20 to 70 MPa and the elongation at break is reduced from 53% to 18% [89]. For electrospun fiber nonwovens acting as scaffold for tissue engineering and prepared from collagen with fiber diameters of about 100 nm moduli of 52 and 26 MPa for elongation along and perpendicular to the orientation direction, respectively, were measured for oriented fiber arrangements with the strength amounting to 1.5 and 0.7 MPa, respectively.

5
Recent Electrospinning Developments

Electrospinning, the resulting nanofibers and nonwovens composed of these nanofibers quite obviously offer unique opportunities in terms of functional nanoobjects and corresponding applications. Yet, despite the richness of features characteristic for electrospinning and the resulting structures the approaches discussed in detail so far may meet with limitations for specific areas of application. Extensions of the basic electrospinning techniques were developed for this reason characterized by other kinds of self-organizations. In particular, these are electrospinning with strongly reduced electrode distances as well as co-electrospinning. Furthermore, electrospun fibers can be used as template to produce hollow fibers.

5.1
Electrospinning with Strongly Reduced Electrode Distances

The patterning of surfaces via a spatially controlled deposition of nanofibers as well as a deposition of nonwovens with well defined geometry and orientation meets with increasing demand. Possible applications include nanofluidics, superhydrophobic patterning, and the integration of nanofibers or nanofiber assemblies into hierarchical structures comprising nanoelectronic or nanophotonic circuits. Among others, current approaches include the design of appropriate counter electrode configurations or the manipulation of the nonwovens composed of such nanofibers once it has been prepared by electrospinning. What is needed is an approach which allows a direct and precise deposition of nanofibers or nanofiber assemblies onto the designated target area.

More recently the so called near field electrospinning was proposed [76–78]. A droplet suspended at an AFM tip is subjected to an electric field existing between the tip and a counter electrode which is located at a distance well below the micrometer range [76]. The droplet is deformed as expected and subsequently deposited in the shape of a rod/short fiber on a moving substrate. The scale is in the nanometer range as the droplet diameter is also in the nanometer range. A further approach involves a microfluidic feeding setup with very fine tips and a rapidly moving take-up substrate [77]. A larger scale technical realization devoted to continuously patterning of extended surfaces or to the continuous incorporation of nanofibers/nanorods into particular nanoelectronic devices is not obvious at this stage.

Another approach working in a continuous fashion – called high precision deposition electrospinning (HPDE) – is based on the experimental die-counter electrode setup used for conventional continuous electrospinning and consists in reducing the distance between the two electrodes from the usual 10–20 cm down to a range extending from 100 μm up to a few millimeters [78]. To induce a continuous spinning process under such conditions, one often has to monitor the spinning process by optical means and to couple the optical signals to the control of the electric field. A reduction in distance will certainly give rise to a decrease of size of the area in which the nonwoven is deposited. Yet, one might also expect that the reduction in electrode distances gives rise to a suppression of the tendency towards the onset of the bending instability and the corresponding strong reduction in fiber diameters. Furthermore, the deposition of wet fibers which subsequently merge to films or are decomposed via Rayleigh instabilities to droplets might lead to problems. The surprising finding was that one becomes able to deposit individual nanofibers or nonwovens in a highly controlled way both in terms of small fiber diameters and of the deposition location and orientation as shown in Fig. 19. Various types of fiber depositions (straight or with loops, with

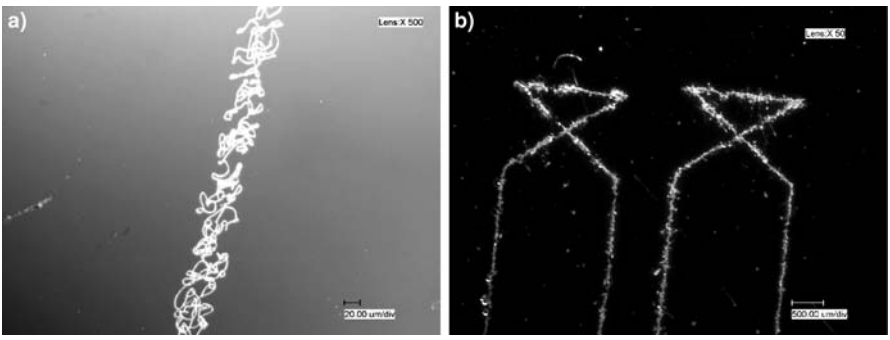

Fig. 19 Precision deposition of nonwoven pattern composed of PEO via the precision deposition approach [78]. **a** Linear trace of nonwoven, **b** Writing of a test pattern

droplets incorporated or without them) can be deposited in a controlled way, and one is able to "write" specific figures, or pattern by moving the substrates accordingly, as also shown in Fig. 19. The expectation is that this type of precision deposition will give rise to novel applications among others in areas relying on surface properties such as sensorics, microfluidics, and possibly the modification of surfaces of implants.

5.2 Co-Electrospinning

Co-electrospinning has been developed to produce core/shell fibers composed of polymer shells and cores, of low molar mass materials as core and a polymer shell, or even hollow fibers. Two dies arranged in a concentric configuration are connected to two reservoirs containing different spinning solutions in this approach. Compound droplets are formed at the tip of the two dies and deformed in the electric field. A compound jet is formed and a compound core-shell fiber is deposited at the counter electrode or substrates located on top of it [90]. The theoretical analysis has revealed that the entrainment of the core droplet may pose a problem. One possible solution is to choose the relative position of the interior die relative to the outer die appropriately [91].

Important features of co-electrospinning with respect to the incorporation of biological objects are: first, that the core can be a low molar mass fluid, including water or oil, providing a natural environment for the biological object, and, second, that the electric charges are located only at the outer surface, so that the inner droplet, and thus biological objects dispersed in it, do not carry charges at all. Yet, they are affected mechanically by the viscous stresses in the jet during spinning. Predictions of these forces are available from theory [91]. The estimate is that biological subjects such as proteins, viruses or bacteria might experience dangerous viscous stresses in specific cases and yet can be adjusted by suitable means to stay moderate.

Co-electrospinning has been applied so far for the preparation of polymer core shell fibers, hollow polymer core shell fibers, hollow fibers composed not only of polymers, but also of ceramics, as well as for the immobilization of functional objects in droplets dispersed in the core that are arranged along the fiber axis. Among the examples reported in the literature are: core shell fibers spun from polystyrene and polyethylene oxide, two kinds of polyethylene oxide (one with and the other without a chromophore), and core shell fibers with the electrically conductive polymer polyhexathiophene and the insulation polymer polyethylene oxide (Fig. 20). Hollow core shell fibers in which one polymer (polycaprolactone) forms the shell onto which the core material is deposited (polyethylene oxide) as inner wall is another example for the broad spectrum of fiber architectures which can be produced by co-electrospinning. The formation of the two-layer hollow fiber is based on the

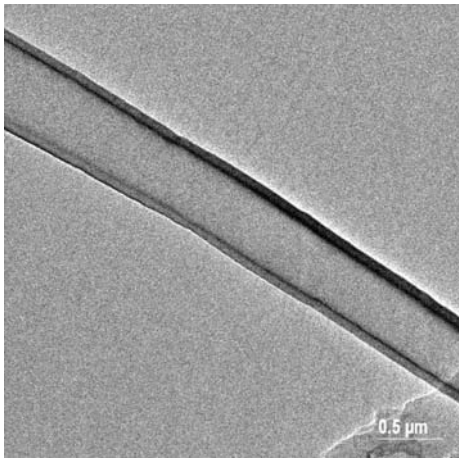

Fig. 20 Core shell nanofibers produced by co-electrospinning PVDF core/PC shell [90]

evaporation of the core solution through the shell yielding the deposition of the core material onto the inner shell layer.

Fluorescent dyes and biological objects such as the green fluorescent protein (GFP) were dispersed in core shell fibers in which the core region consists of water and the functional units. The architecture may be characterized in this case by droplets that are regularly arranged along the fiber axis as pearls in a necklace [92, 93]. Such fibers can be used, for instance, for sensorics: the GFP reversibly looses its capability to display fluorescence if in contact with denaturizing compounds such as urea. Furthermore titanium hollow fibers were produced using in this case a precursor route. The core materials were chosen to be a mineral oil, and the shell material consisted of a mixture of polyvinylpyrrolidone and the precursor compound TiO [94]. The removal of the oil from the core shell fibers followed by a calcinations step yields titanium hollow fibers.

The interest in co-electrospinning is continuously increasing, while applications related to tissue engineering, microfluidics, optoelectronics, and sensorics are being discussed in the literature. It should finally be pointed out that a coaxial jet generation has already been considered previously in the context of electrospraying of compound droplets [95].

5.3 Core Shell Fibers and Hollow Fibers via Templates (TUFT Approach)

Another concept on how to produce core shell fibers or hollow fibers is based on the exploitation of electrospun nanofiber as a template (TUFT: tubes by fiber templates) onto which a second material is deposited as shell either from solution or melt, via layer by layer techniques or from the vapor

phase [96–99]. It is frequently preferable to apply the shell from the vapor phase rather than from a fluid phase since the latter may give rise to mechanical forces causing a disruption of the tiny template fibers towards an inhomogeneous coating or to a swelling of the template disturbing the original dimension of it.

Metals, glasses, or ceramics have been deposited as shell material from the vapor phase onto the template fiber and polymers, though the vapor phase deposition is limited in this case to very special polymers. Examples are polyparaxylylene (PPX) and its derivatives. A precursor, paracyclophane, and corresponding derivatives are pyrolized at 650 °C in this case yielding activated monomers which polymerize on deposition at room temperature on a substrate. One particular feature of the TUFT approach is that several layers of different materials can be deposited yielding nanofibers of complex architecture. The core shell fibers can be functionalized by incorporating nanoparticles and functional molecules such as chromophores, drugs, or catalysts into the core fiber via electrospinning. The shell layer is then being used either to control the kinetics of delivery of the functional molecules or to immobilize them, at the same time allowing them access to the functional molecules from the environment (see below). PPX has particular advantages as shell material for such applications, since it is insoluble in most solvents even at higher temperatures; yet, specific molecules are able to diffuse through PPX-layers via the amorphous regions.

To obtain hollow fibers the core fiber is removed by thermal decomposition, selective solvents or by biodegradation. The internal surface of the hollow fibers is structured in this case by the surface topology of the template fibers. Porous template fibers, for instance, give rise to hollow fibers showing an internal assembly of spikes. Among other reasons, this is of interest for microfluidic applications, since these spikes will affect both the wetting

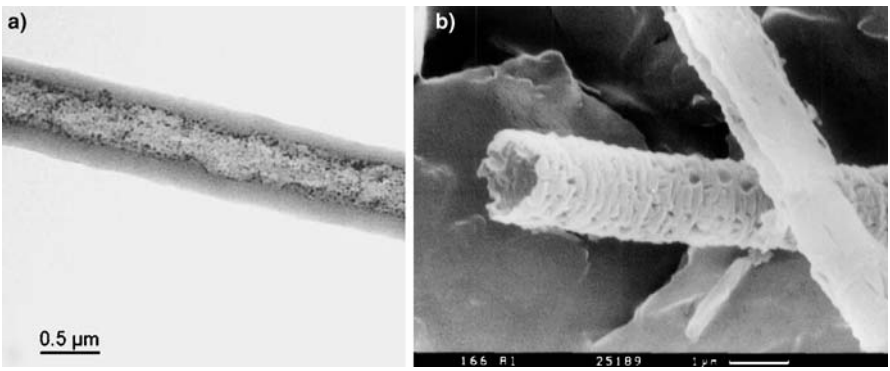

Fig. 21 **a** Hollow fibers composed of PPX and palladium nanoparticles produced via the TUFT-approach [99], **b** Aluminium oxide hollow fibers

of the nanotubes by a given fluid and its transport through the nanotube. Using the TUFT approach hollow fibers made from polymers and metals such as aluminum, chromium, copper, gold, nickel, and others composed of titanium dioxide have been prepared (Fig. 21). Titanium tetraisopropylate was deposited in another example as precursor material onto a polyamide template fiber, the template fibers were pyrolized, and the precursor was calcinated yielding titanium dioxide [98]. It is obvious that the TUFT-approach broadly extends the range of applications of electrospun fibers.

6
Brief Review of Materials Which have been Electrospun to Fibers

6.1
Spinning of Technical Polymers

Electrospinning is currently applied predominantly to polymers of synthetic and natural origin. The major reason is that polymer solutions and polymer melts possess specific flow properties that support the fiber forming process in electrospinning taking place via self-assembly. These flow properties have their origin in the particular conformation of long chain molecules – statistical Gaussian coils have sizes of the order of several 10 nm (as far as long flexible chain molecules are concerned) – and their interaction with each other via entanglements in melts or more concentrated solutions [100, 101]. Such chain entangled fluids are characterized by very unique viscoelastic properties [37], and they are, in turn, able to sustain the strong elongational strains, strain rates and the looping and spiraling pathways characteristic of the bending instability in electrospinning without rupture. A decrease of the molecular weight of a given polymer decreasing towards oligomers, keeping the spinning parameters constant, tends to give rise to the formation of beaded fibers rather than smooth fibers and finally, if the molecular weight is further decreased, to the formation of just droplets. Experimental methods are available – also on a commercial basis – allowing one to determine the viscoelastic response, viscoelastic relaxation times of polymer melts, and, in particular, of polymer solutions. The analysis is based on the time-dependent changes in the diameter of a fluid meniscus located between two plates [37].

6.1.1
Spinning from Polymer Melts

Electrospinning can obviously be applied to both the viscoelastic molten state as well as to the viscoelastic solution state. Yet, so far only a very small number of the studies have been published in the literature considering elec-

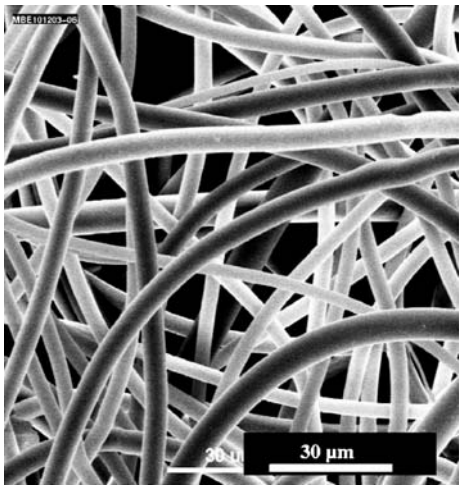

Fig. 22 PA 6 nanofibers produced by melt electrospinning [106]

trospinning from the molten state [102–106]. This holds despite the fact that two topics of great technical importance, i.e., the need to get rid of the large amount of solvents involved in solution electrospinning and the need to increase the production rate, are met by melt electrospinning. The problem which melt spinning still encounters is that the resulting fibers tend to possess diameters well outside the nanometer range, i.e., of the order of a few micrometers up to several 10 µm. The high viscosity and the peculiar viscoelastic properties of melts as controlled by the exceedingly dense entanglement network formed by the polymer chains are two reasons for this problem. Electrospinning has, in any case, to be performed at elevated temperatures well above the respective melting or glass transition temperatures. Strong electric fields are beneficial in this context and, in fact, electrospinning has been done even in vacuum or in the presence of electrically protective gases such as SF_6 to achieve an electrical field as high as possible without encountering an electric breakthrough.

Polypropylene, polyamide 12, polyethylene terephthalate, polyurethane, polycaprolactone polyamide 12 are examples of polymers which have been electrospun from the melt. In general the fibers' diameters are still in the micrometer range with PA 6 fiber diameters known today to be as low as 900 nm. Fibers with diameters even down to about 300 nm and below were more recently reported for the electrospinning of a low melting polycaprolactone [105]. A reduction of molecular weights seems a promising approach although properties of the solid materials tend to become poorer in this case. Nevertheless these results indicate that one may be able to produce nanofibers from polymer melts by tailoring polymer melt properties appropriately, for instance, via a careful selection of the molecular weight and its distribution

as well as of the processing temperature relative to the glass transition or melting temperature. It is obvious that melt electrospinning is still in its infancy. The progress which has been made recently nevertheless indicates that one will succeed in the near future to produce electrospun fibers from the melt with diameters down to a few 100 nm and even below. This would give a major push to technical applications of electrospun nanofibers.

6.1.2 Electrospinning from Organic Solvents

Electrospinning from polymer solutions can be much more easily controlled, since the viscoelastic properties, surface tension, or even electric conductivity can be modified via the choice of the solvent, solvent mixture, the polymer concentration in the spinning solution, the temperature of the spinning solution, and, in particular cases, also via specific additives. It has been demonstrated that polymer fibers with diameters created to a few nanometer can be achieved by a suitable choice of the spinning parameters. An extremely broad range of technical, functional synthetic and natural polymers has thus been spun to nanofibers and the number of novel polymer systems produced as nanofibers is ever increasing [9–13].

Among the large number of polymers that have been electrospun from organic solvents to nanofibers are polystyrene (PS), polyacrylonitrile (PAN), polycarbonate (PC), aliphatic and aromatic polyamides (PA), polyimides (PI), polybenzimidazol (PBI), poly(ethylenterephthalate) (PET), poly(trimethylenterephthalate) (PTT), poly(hexamethylenterephthalate-*co*-hexamethylen-2,6-naphthalate) (P(HT-co-HN)), polyurethanes (PU), poly(ethylene-*co*-vinylacetate) (PEV), polyvinylchloride (PVC), polymethylmethacrylate (PMMA), polyvinylbutyral (PVB), cellulose acetate (CA), polyvinylidenfluoride (PVDF), and many more as detailed in several review papers [9–13]. Poly-(*p*-phenylenterephthalate) (PPTA) also known under the trade names Kevlar and Twaron) is an aromatic polyamide that cannot be melted without decomposition, yet it can be electrospun from appropriate solvents and at sufficient concentrations for which lyotropic solutions are formed, yielding fibers with extremely high tensile strengths. Other polymers with high thermal stability that cannot be melted without decomposition are PI and PBI. These polymers can be prepared as nanofibers via electrospinning of soluble precursors, which are subsequently transformed to the polymer species by polymer analogous reactions. Electrospinning of polyacrylonitrile fibers has been considered in detail. One reason for this consideration is that they can be converted into carbon fibers by pyrolysis. With electrospinning of poly(ferrocenyldimethylsilane), it was possible to show that organometallic polymers can also be spun into very fine fibers.

The advantage of electrospinning from organic solvents is the broad scope of polymer systems soluble in organic solvents. Disadvantages are, as pointed

out above, the properties of the organic solvents themselves, such as flammability, toxicity, corrosiveness, disposal, etc. These disadvantages may not be an issue on a laboratory scale but will play a major role in industrial production setups. Spinning of fibers from water soluble polymers constitutes a major benefit in this respect.

6.1.3 Electrospinning of Water Soluble Polymers

Water is an ecologically preferable and safe solvent, its solubility can be adjusted by variations of the pH-value or the temperature, for instance. A major disadvantage is, of course, that fibers composed of water soluble polymers tend to decompose rapidly upon contact with water. While this may be positive for biomedical applications, additional stabilization of these fibers, among other techniques, by cross-linking, is necessary for other technical applications, such as filters or textiles.

Extensive investigations have been carried out on water soluble polymers such as polyethylene oxide PEO, polyvinylacetate PVA, poly(acrylic acid) (PAA), poly(acrylic amide), polyelectrolytes, poly(vinylpyrrolidon) (PVP), and hydroxypropylcellulose (HPC). PEO is especially versatile, because it is also soluble in many organic solvents. Therefore, it can be electrospun from a variety of solvents. Compared to PEO polyvinylalcohol offers an even larger scope of variations. Starting from polyvinylacetate the degree of hydrolization of PVA can be adjusted and thus the solubility of the polymer in water. The hydroxy groups present in PVA can be used either before or after electrospinning to create chemical reactions for multiple purposes. PAA can be electrospun from aqueous solution almost just as well as PVA. Further modifications are possible by variation of pH-values and addition of salts, respectively. The physical stability of PVA/PAA blends towards water can be significantly improved by chemical cross-linking reactions. The water resistance of electrospun PVA/PAA blend fibers can be increased by analogous esterification reactions or by aldol reactions with polyaldehydes. An interesting alternative to cross-linking of PVA with PAA or polyaldehydes can be achieved with electrospun PVA/cyclodextrin fibers that show a strong pH-dependent swelling behavior versus water after thermal cross-linking. Chemical cross-linking of electrospun PVA derivatives can also be accomplished for PVA functionalized with photo-crosslinkable substituents via exposure to light.

One alternative for the cross-linking of electrospun fibers is the so-called "reactive electrospinning". In an example a mixture of 2-hydroxymethylmethacrylate, methacrylic acid, ethylenglycoldimethacrylate, 2,2′-diazo-*iso*-butyronitril and a photo cross-linking agent were first pre-polymerized and subsequently photochemically cross-linked during the electrospinning process. Following a similar concept poly(dicyclopentadien) fibers can be ob-

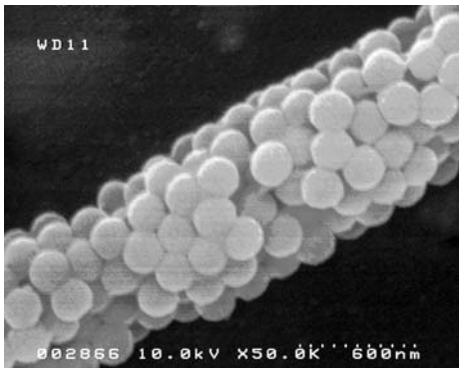

Fig. 23 Nanofibers based on polystyrene latex particles spun from water dispersions yet being water insoluble as electrospun fibers

tained by "reactive electrospinning". Finally, polyvinylpyrrolidone, which can also be electrospun from aqueous solution, was used to produce structured electrospun fibers by spinning of PVP blends and subsequent selective extraction.

A highly interesting route towards water stable nanofibers using water as solvent is based on colloidal dispersions of polystyrene latex particles [107]. To obtain fibers during electrospinning a water soluble polymer such as PVA has to be added to the spinning solution in low concentrations (typically about 6 wt. %), which is subsequently removed after fiber formation by rinsing the fibers in water. The latex particles fuse within the spun fibers yielding water insoluble nanofibers. Figure 23 shows the resulting fibers, which in fact are no longer soluble in water. It is very obvious that the fibers are composed of nanoscalar spheres. This approach can be extended to other types of polymer species.

6.2 Spinning of Biopolymers

Electrospun nanofibers, nonwovens composed of biopolymers are of ever growing interest in medicinal applications, including surface modifications of implants, tissue engineering, wound healing, and drug delivery. Some of these areas will be discussed below in more detail. A set of biopolymers, modified biopolymers, and their blends with synthetic polymers were processed into nanofibers by electrospinning often only under very specific conditions, such as using special solvents or processing these materials as blends with synthetic polymers such as PEO or PVA.

Collagen can be electrospun from hexafluoroisopropanol or as blend with PEO, PCL, and PLA-co-PCL leading to collagen fibers with diameters of 200 to 500 nm and denatured collagen, so-called gelatin, from aque-

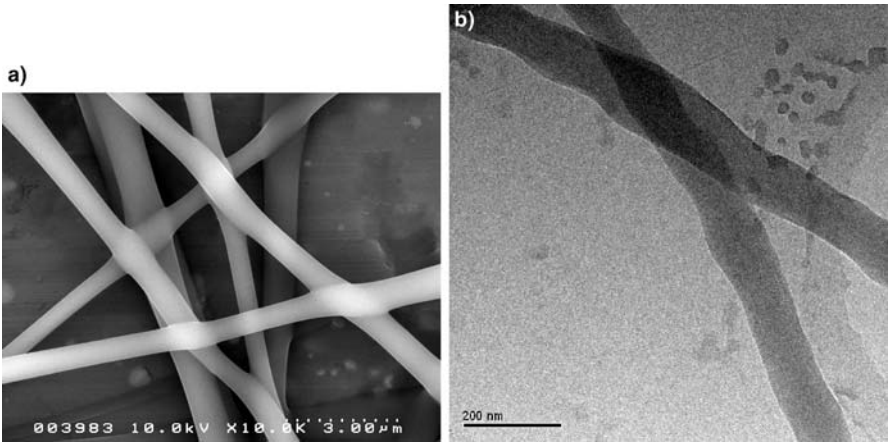

Fig. 24 Nanofibers from: **a** Collagen, **b** Chitosan

ous solution and trifluorethanol, respectively, as pure polymer or as blend (Fig. 24a) [108]. Chitin and chitosan can be electrospun to nanofibers in its pure form and as blends as well (Fig. 24b) [109]. These fibers are of particular interest for wound dressings. Other proteins and enzymes such as casein, lipase, cellulose, bovin serumalbumin, and luciferase can only be processed by electrospinning as blends with synthetic polymers. A series of papers have described electrospinning of silk and silk-like polymers mainly for biomedical applications [110]. Cellulose as classic fiber material can be electrospun from *N*-methylmorpholin-*N*-oxide/water systems, and dimethyl acetamide/LiCl systems, respectively, into fibers with diameters in the submicrometer range. Cellulose acetate as organosoluble cellulose derivative and well established filter material was electrospun to fibers without any problem.

Polymers which can be hydrolyzed under physiological conditions or are biodegradable (summarized as bioerodible polymers), such as aliphatic polyesters, polyanhydrides, polyphosphazenes, etc., are very important for a large variety of applications. Electrospun fibers of such bioerodible polymers are intensely studied for pharmaceutical applications or for the field of regenerative medicine (tissue engineering). Polylactide (PLA), an aliphatic polyester, is one of the classical bioerodible polymers that were successfully electrospun. One reason for the easy processing of the different PLA isomers by electrospinning is their high solubility in halogenated aliphatic solvents. Polyglycolid, in contrast, was used in electrospinning processes only to a minor degree. Poly(ε-caprolactone) (PCL), which is easily soluble in different solvents, and PCL copolymers were extensively used for fabrication of electrospun scaffolds. An interesting alternative to PLA and PCL are poly(hydroxybutyrate)s and their derivatives.

6.3
Nanofibers from Polymer Hybrids, Metals, Metal Oxides

Nanofibers/nanowires composed of nonpolymeric materials, such as metals, metal oxides meet with strong interest for applications in nanoelectronics, nanooptics or nanomagnetism due to the specific dependence of their properties on the 1-d character of fibers, on the diameter of the fibers, and on their axial ratio [111–113]. Various methods are now available to produce nanowires including among others electron beam methods, interferometric lithography, microprobe assisted manipulations, or electrodeposition into porous templates, such as aluminum templates prepared by electrochemical approaches or into blockcopolymers [112]. Disadvantages, however, of these methods include that they are in the majority of cases time consuming, expensive, and that the yield in terms of the weight or volume of the nanowires that can be produced is very limited. Electrospinning offers, in principle, a highly attractive alternative.

Yet, a major problem as far as the application of this technique for the production of metal or oxide fibers for that matter is that – as already pointed out above – solution or melt appropriate for electrospinning should display specific viscous, in particular viscoelastic properties. Such specific rheological properties are natural for polymer materials and it is for this reason that the majority of papers dealing with electrospinning have concentrated on polymer materials. Yet, electrospinning can be exploited for the preparation of metal, metal oxide, semiconductor nanowires and of the corresponding polymer hybrids following the precursor route. Precursors of the target materials such as metal salts are introduced for this purpose into spinning solutions containing polymers and an appropriate solvent able to solve both the polymer and the salts. Electrospinning of such a ternary solution is found to give rise to polymer nanowires in which the salts are homogeneously dispersed provided that the spinning parameters are chosen appropriately.

The precursor materials are, in a subsequent step, reduced to the target metals or metal oxides via thermal treatment or the treatment in the presence of reducing agents such as hydrogen. The results are polymer hybrid nanofibers. In a further step the polymer can be removed completely, in general again by thermal treatment, for example, to yield nanofibers from the pure metal or metal oxide material. All of these steps can be done on a technical scale yielding sizable amounts of nanowires.

6.3.1
Polymer Hybrids

Polymer hybrid nanofibers in which nanoparticles, composed of platinum, rhodium, and palladium, are dispersed were prepared along the precursor

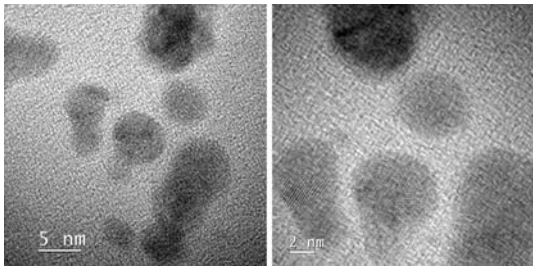

Fig. 25 Rhodium-palladium bimetallic nanoparticles for catalytic applications grown within the nanofibers via the precursor route [114, 115]

route using appropriate salts, aiming at heterogeneous catalysis [114, 115]. To obtain bimetallic particles the spinning solution has to be composed of the two corresponding precursor salts in addition to the polymer species and the solvent. The reduction yields nanoparticles within the polymer nanofiber with diameters typically in the 3–5 nm range, which are again highly dispersed (Fig. 25). An EDX analysis revealed that all bimetallic particles observed by TEM are composed of the two metals in the ratio defined by the concentration of the precursor salts in the original spinning solution. An interesting feature of the approach described here is that bimetallic nanoparticles become available with compositions that are not accessible on a macroscopic scale for which the observed compositions are located well within the binodal regime. Catalytic test reactions with such polymer nanofibers were highly successful.

In a similar way polymer hybrid nanofibers were produced containing nanoparticles with either ferromagnetic or superparamagnetic properties [115–117]. Fe_3O_4, for example, is a well known ferrimagnetic material

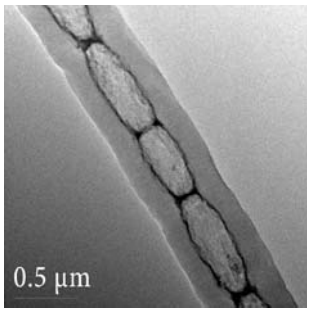

Fig. 26 Compartimented nanofibers composed of PPX with superparamagnetic iron oxide particles at interfaces [115]

which, however, becomes superparamagnetic as the size of the particles is reduced down to the nm-scale. Superparamagnetism is characterized by a very high magnetization in the presence of an external magnetic field, yet the magnetization is not permanent and no hysteresis effects characteristic of ferromagnetism are observed. Highly interesting morphologies are developed if the original nanofiber is coated by PPX using the TUFT-approach in order to stabilize the nanofibers mechanically and thermally, and if the reduction is subsequently performed at an elevated temperature [115]. The polylactide melts in the selected temperature range; the polylactide core fiber then tends to fragment into nanodroplets via the well known Rayleigh instabilities. The final result is a compartmented fiber as shown in Fig. 26 in which the nanoparticles have accumulated on the surface of these droplets. This enrichment of nanoparticles at interfaces – colloidal jamming – has been the subject of several papers in the literature. The fibers nevertheless display superparamagnetism despite the agglomeration at interfaces due to their separation by polymer sheets.

6.3.2
Metal and Metal Oxide Nanofibers

Metal/metal oxide nanofibers become available if one succeeds in dispersing high amounts of the precursor species in the spinning solutions well above a weigh ratio precursor/polymer of 50% up to 80% and more [115, 118, 119]. The preparation of nanofibers composed of copper is an example. Copper nitrate was chosen as precursor salt. It was dispersed in a spinning solution containing the solvent mixture water/isopropanol and polyvinyl butyral as polymer component. Electrospinning gave rise to homogeneous nanofibers with diameters in the 550 nm-range. The thermal reduction and a subse-

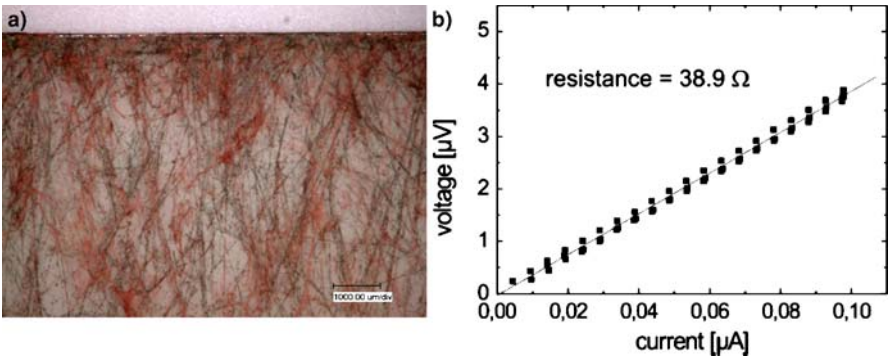

Fig. 27 **a** Nanofibers composed of Cu prepared via the precursor route and **b** single fiber current/voltage characteristics [118]

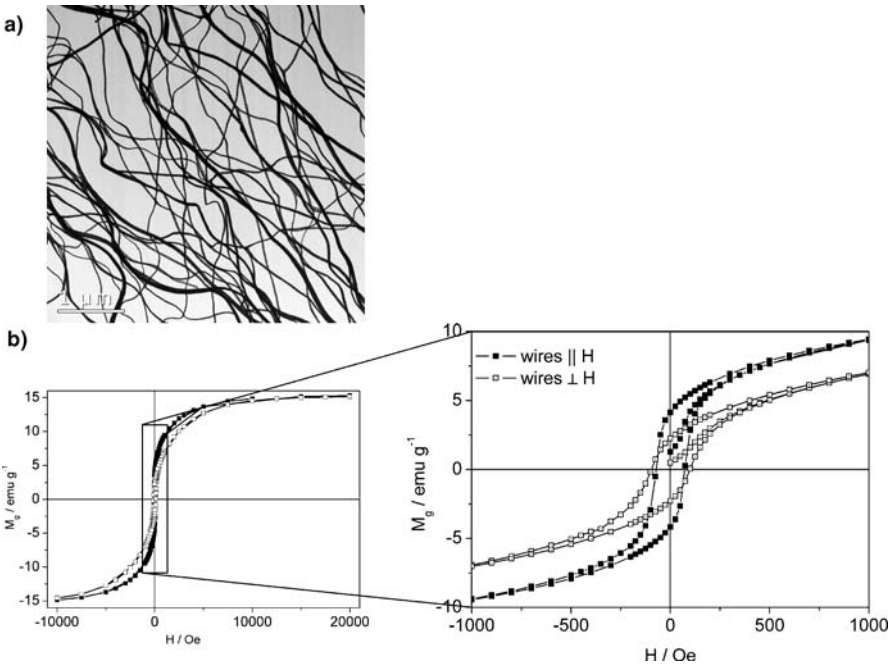

Fig. 28 **a** Co nanofibers and **b** Anisotropic magnetization diagram of ferromagnetic Co nanofiber [115, 119]

quent reduction in the presence of hydrogen yielded nanofibers composed of pure copper (Fig. 27) displaying the reddish color characteristic of copper and the X-ray analysis showed the crystal structure characteristic of copper. The diameter of the copper nanofibers amounted to about 270 nm, which is well below the diameter of the original fiber primarily due to the loss of the polymer component. Electrical conduction investigations revealed a specific conductance of $8.5 \times 10^3\ \Omega^{-1}\ \mathrm{cm}^{-1}$.

In a similar way nanofibers composed of nickel, iron, iron oxides, or cobalt were prepared, displaying specific magnetic properties [115, 119]. Cobalt nanowires are shown in Fig. 28, as an example, the radius being controlled from below 20 nm up to several 100 nm depending on the salt loading of the spinning solution. Nanofibers composed of ferromagnetic materials are expected to show ferromagnetism rather than superparamagnetism even for very small fiber diameters, since they are elongated in one dimension well above the nanometer-scale [112, 113] and in fact they display anisotropic magnetization diagrams as shown in Fig. 28. The hysteresis displays different shapes for the magnetic field oriented along the fiber axis as compared to the perpendicular case.

7
Applications for Electrospun Nanofibers

7.1
Technical Applications

The spectrum of applications that can be envisioned for electrospun nanofibers is extremely broad due to their unique intrinsic structure, surface properties, and functions. Applications both related to Material Science and Life Science areas will be discussed in the following, though only briefly since the focus of this contribution is primarily on the processes controlling nanofiber formation in electrospinning by self-organization processes. For each of the applications mentioned in the following the specific set of features of electrospun fibers of particular benefit for this application will be pointed out.

7.1.1
Template Applications

Electrospun polymer fibers can be used as examples for the preparation of hollow fibers (tubes by fiber templates process = TUFT process) (e.g., see [97–100]). According to the TUFT process electrospun biodegradable or soluble polymer fibers are coated with polymers, metals or other materials. After selective extraction or degradation of the template fibers hollow fibers whose dimensions depict the negative replication of the template fibers are obtained. Au, Cu and Ni hollow fibers were fabricated in an analogous way. In a further development of the TUFT process hollow fibers with intricate architectures were prepared by electrospinning using the layer by layer technique. Both, the magnitude of the inner diameter as well as the surface topology of the interior wall are controlled by the template fiber properties, and the template fiber allows the introduction of functional materials into the hollow fibers.

7.1.2
Textile Applications

Nanofiber based nonwovens can be used to strongly modify the properties of conventional textiles composed of much thicker textile fibers (e.g., see [121,122]). The nanofibers allow a great increase in wind resistance, ability to adjust water vapor permeability, optimize thermal isolation behavior, and to prepare textiles with special functionalities (such as the self-cleaning (lotus) effect, aerosol filtering, and protection against chemical or biological hazards). Features which control these functions are predominantly the intrinsic pore structures, the corresponding permeation properties for gases and fluids, and the high specific surface area that comes with the nanodimensions.

7.1.3
Filter Applications

High filter efficiencies rely on the fact that the channels and pores within the filter material can be adjusted to the fineness of the particles which are supposed to be filtered out. By the transition from fibers with diameters in the μm range to fibers with diameters in the nm range one becomes able to filter finer and finer particles (e.g., see [122,124]). Coalesence and aerosol filters are characteristic applications for nanofiber nonwovens. Very recently aerosol filtration was simulated for nanofiber filters concentrating on reduced operating pressures [123]. It was pointed out in this paper that the flow lines around nanofibers may differ strongly from the ones around μm-sized fibers, in which case the free molecular flow regime may become dominant. Important results of the simulations are that the collection efficiency of the nanofiber filters increase strongly with decreasing fiber diameter at constant pressure drop and that the diameter of the particle which can be captured with high efficiency also decreases strongly with decreasing fiber diameter. Furthermore, for gas filters a transition from depth filtration to surface filtration can be induced which allows the filter to be cleaned by reverse pressure pulses very effectively increasing the lifetime of such a filter by up to a factor of 10.

7.1.4
Catalysis

A huge problem in catalysis is the removal and recycling of the catalytic agent after the reaction (e.g., see [115,116,125]). The implantation of homogeneous as well as heterogeneous catalysts into nanofibers poses an interesting solution for these problems. The reaction mixture can circulate around the fibers as is the case in the continuously working microreaction technique, or the fibers fixed on a carrier can be immersed repeatedly into a reaction vessel to catalyze the content of the vessel. Short diffusion distances within nanofibers and the specific pore structures and high surface areas of nanofiber nonwovens allow rapid access of the reaction components to the catalysts and of the products back into the reaction mixture.

7.1.5
Nanofiber Reinforcement

Fiber reinforcement is controlled primarily by the mechanical properties of the fibers, their axial ratio, and the mechanical coupling between the fibers and the matrix (e.g., see [126]). Electrospun nanofibers tend to display enhanced mechanical properties due to the self-organization controlling fiber formation during electrospinning. Furthermore, the axial ratio of the fibers, nanofibers with diameters of about 10 or 100 nm, can be 100 to 1000 times

shorter than for fibers with diameters in the range of 10 to 100 μm. Due to their small diameters nanofibers cause only negligible refraction of light so that transparent matrices, which are reinforced by nanofibers, stay transparent, even if the refraction indices of matrix and fibers do not match. Finally, the large specific surface between nanofiber and matrix enhances relaxation processes, which improves the impact strength of the strengthened matrix.

7.2 Medicinal Applications

7.2.1 Tissue Engineering

Tissue engineering aims at artificially growing diverse types of tissues used to replace corresponding tissues destroyed by an accident or illness in the human body (e.g., see [127]). Cartilages, bones, skin, blood vessels, lymphatic vessels, lungs, and heart tissue are targets for this kind of reconstruction. One – in vitro or in vivo – approach in the field of tissue engineering is based on the use of scaffolds onto which cells or human body cells, respectively, can be settled. The scaffold has to facilitate anchorage, migration, and proliferation of the cells, to provide the three dimensional structure model of the tissue, and it has to fulfill a diverse range of requirements concerning biocompatibility, biodegradability, architecture, sterilizability, porosity, incorporation and release of drugs, mechanical properties, etc. Scaffolds based on nanofiber nonwovens and composed of synthetic biocompatible polymers or of natural ones, such as collagen, are highly promising. A major reason for this promise is that this approach allows the scaffolds to mimic the architecture of the extracellular matrix enclosing the cells in tissues. Furthermore, functional components such as growth factors can be incorporated via electrospinning.

7.2.2 Wound Healing with Nanofibers

An interesting application of nanofibers and especially electrospinning as a method to produce such nanofibers is in the treatment of large wounds, such as burns and abrasions. Observations are that these kinds of wounds heal particularly fast and without complications if they are covered by a thin web of nanofibers especially from biodegradable polymers (e.g., see [128]). Such nanowebs provide enough pores for an exchange of liquids and gases with the environment, but the pores are dimensioned in such a way that no bacteria can enter. Electrospun nanofiber nonwovens generally show very good adhesion even to moist wounds. Furthermore, the previously men-

tioned large surface of up to 100 m^2 per gram is highly beneficial for liquid adsorption and local release of drugs on the skin. In contrast to conventional wound treatment nanofibers also prevent scarring.

7.2.3 Transport and Release of Drugs/Drug Delivery

Nanofiber systems for the release of drugs or other functional compounds are generally not only of interest for wound healing or tissue engineering. Nanostructured systems for tumor therapy and also for other types of therapies like inhalation therapy or pain therapy are currently investigated worldwide (e.g., see [129,130]). In an ideal case, they have to fulfill versatile jobs in this function. The nanoobjects are supposed to protect the drugs in the case of systemic application from decomposition, e.g., in the blood circuit. Furthermore they should allow controlled release of the drug at a release rate as constant as possible over a longer period of time, adjusted depending on the field of application. They have to be able to permeate certain membranes or barriers, e.g., the blood–brain barrier, and they are supposed to concentrate the drug release only on the targeted body area.

Electrospun nanofiber may serve in this context as carriers for drugs and as controlled release agent. The domain of nanofibers loaded with drugs will most likely be of little importance for systemic therapy but of great importance for loco-regional therapy, i.e., the fibers are localized at the exact part of the body that is supposed to be treated with the carried drug. A currently developing field of application is inhalation therapy based on nanorods. The reason for this application is that the aerodynamic radius of such rods can be adjusted via the dimension of the rods in such a way that the drug carriers can be deposited at specific positions in the lung. It is well known from extensive experimental and theoretical studies correlated with the asbestos problem how fiber-shaped particles are deposited in the lung as a function of their axis ratio, length, radius, density, and surface structure [130, 131]. This knowledge can be used to place rod-shaped drug carriers at specific positions in the lung for loco-regional release. An advantage of using rodlike instead of spherical drug carriers is that the percentage of rods that remains in the lung after inhalation and is not exhaled is significantly higher than in the case of spherical particles. The treatment of tumors, metastases, pulmonary hypertension, and asthma, as well as the administration of insulin or other drugs via the lung are current research goals.

To be able to selectively adjust the aerodynamic diameters, the nanofibers fabricated by electrospinning have to be shortened to a defined axis ratio. This task can be achieved by laser or mechanical cutting. To control the aerodynamic radius via the density, highly porous fibers may be used. Inhalation therapy will have to be based on polymers which are biocompatible with particular emphasis on the specific reactions within the lung.

Acknowledgements The authors would like to thank Dr. Roland Dersch, Dr. Max von Bistram and Dr. Martin Graeser for their valuable support in the preparation of the manuscript. Financial support from the Deutsche Forschungsgemeinschaft (DFG) and the Volkswagen foundation is gratefully acknowledged.

References

1. Langer RM (1969) Integ Comp Biol 9:81
2. Wallenberger FT, Weston NE (2004) Natural fibers, plastics and composites. Springer, Heidelberg
3. Yang HH (1989) Aromatic high strength fibers. Wiley, New York
4. Cabasso I, Klein E, Smith JK (1976) Appl Polym Sci 20:2377
5. Folkes MJ (1982) Short fiber reinforced thermoplastics. Wiley, New York
6. Shin C, Chase GG (2004) AIChE J 50:343
7. Lee Y, Wadsworth LC (1992) Polymer 33:1200
8. Hagewood J, Wilkie A (2003) Nonwovens World 12:69–73
9. Huang ZM, Zhang YZ, Kotaki M, Ramakrishna S (2003) Compos Sci Technol 63:2223
10. Dersch R, Greiner A, Wendorff JH (2004) In: Schwartz JA, Contesen CJ, Putger K (eds) Dekker Encyclopedia of Nanoscience and Nanotechnology. Marcel Dekker, New York, p 2931
11. Li D, Xia Y (2004) Adv Mater 16:1151
12. Greiner A, Wendorff JH (2007) Angew Chem Int Edit 119:5750
13. Reneker DH, Yarin AL, Zussman E, Xu H (2007) Adv Appl Mechanics 41:44
14. Barrero A, Loscertales IG (2007) Ann Rev Fluid Mech 39:89
15. Marin AG, Loscertales IG, Marquez M, Barrero A (2007) Phys Rev Lett 98:014502
16. Lehn M (1990) Angew Chem Int Edit 11:1304
17. Vriezema DM, Aragones AC, Elemans AAW, Cornelissen JLM, Rowan AE, Nolte RJM (2005) Chem Rev 105:1445
18. Earnshaw S (1842) Trans Camb Phil Soc 7:97
19. Reneker DH, Yarin AL, Fong H, Koombhongse S (2000) J Appl Phys 87:4531
20. Yarin AL, Koombhongse S, Reneker DH (2001) J Appl Phys 90:4836
21. Reznik SN, Yarin AL, Theron A, Zusmann E (2004) J Fluid Mech 516:349
22. Yarin AL, Zussman E (2004) Polymer 45:2977
23. Larrondo L, Manly RSJ (1981) J Polym Sci Polym Phys 19:921
24. Xu H, Yarin AL, Reneker DH (2003) Polym Prepr 44:51
25. de Gennes P (2003) J Chem Phys 60:5030
26. Warner SB, Buer A, Ugbolue SC, Rutledge GC, Shin MY (1998) Nat Textile Center Annual Rep No 83
27. Lord Rayleigh X (1882) Philos Mag 44:18
28. Zeleny J (1917) Phys Rev 10:1
29. Taylor G (1964) Proc R Soc London A 280:383
30. Yarin AL, Koombhongse S, Reneker DH (2001) J Appl Phys 89:3018
31. Hohman MM, Shin M, Rutledge G, Brenner MP (2001) Phys Fluids 13:2201
32. Hohman MM, Shin M, Rutledge G, Brenner MP (2001) Phys Fluids 13:2221
33. Shin YM, Hohmann MM, Brenner M, Rutledge GC (2001) Polymer 42:9955
34. Fridrikh SV, Yu JH, Brenner MP, Rutledge GC (2001) Appl Phys Lett 78:1149
35. Fridrikh SV, Yu JH, Brenner MP, Rutledge GC (2001) Phys Rev Lett 90:144502
36. Yarin AL, Kataphinan W, Reneker DH (2005) J Appl Phys 98:064501

37. Stelter M, Brenn G, Yarin AL, Singh RP, Durst F (2000) J Rheol 44:595
38. Holzmeister A, Greiner J, Wendorff JH (2007) Eur Polym J 43:4859
39. He JH, Wan YQ, Yu JY (2004) J Nonlinear Sci Numer Simul 5:253
40. Wan YQ, He JH, Yu JY, Wu Y (2006) J Appl Polym Sci 103:3840
41. Fridrikh SV, Yu JH, Brenner MP, Rutledge GC (2003) Phys Rev Lett 90:144502
42. Baumgarten K (1971) J Colloid Interf Sci 36:71
43. Theron SA, Zussman E, Yarin AL (2004) Polymer 45:2017
44. Hou H, Jun Z, Reuning A, Schaper A, Wendorff JH, Greiner A (2002) Macromolecules 35:2429
45. Koombhongse S, Liu WX, Reneker DH (2001) J Polym Sci B 39:2599
46. Ma M, Gupta M, Li Z, Zhai L, Gleason KK, Cohen R, Rubner MF, Rutledge GC (2007) Adv Mater 19:255
47. Lord Rayleigh X (1892) Phil Mag 34:145
48. Tomotika S (1935) Proc R Soc London A 150:322
49. Higgins JS, Tambasco M, Lipson JEG (2005) Prog Polym Sci 30:832
50. McCann J, Marquez M, Xia Y (2006) J Am Chem Soc 128:1436
51. Casper CL, Stephens JS, Tasi NG, Rabolt JF (2004) Macromolecules 37:573
52. Megelski S, Stephens JS, Bruce CD, Rabolt JF (2002) Macromolecules 35:8456
53. Bognitzki M, Czado W, Frese T, Schaper A, Hellwig M, Steinhart M, Greiner A, Wendorff JH (2001) Adv Mater 13:70
54. Vogt M (2006) Diploma Thesis, Philipps University, Marburg
55. Weisbuch C, Vinter B (2007) Quantum Semiconductor Structures. Academic Press, New York
56. Struik LCE (1977) Polym Eng Sci 17:165
57. Efremov MY, Olson EA, Zhang M, Zhang Z, Allen LH (2004) Macromolecules 37:4607
58. Efremov MY, Olson EA, Zhang M, Zhang Z, Allen LH (2004) Phys Rev Lett 91:085703
59. Agarwal S, Puchner M, Greiner A, Wendorff JH (2005) Polym Int 54:1422
60. Kim JS, Reneker DH (1999) Polym Eng Sci 39:849
61. Strobl G (1997) The Physics of Polymers. Springer, Berlin
62. Kim JS, Lee DS (2000) Polym J 32:616
63. Dersch R, Liu T, Schaper A, Greiner A, Wendorff JH (2003) Polym Sci A 41:545
64. Stephens JS, Chase DB, Rabolt JF (2002) Macromol 37:877
65. Dersch R (2002) Diploma Thesis, Philipps University, Marburg
66. Chen Z, Foster MD, Zhou W, Fong H, Reneker DH (2001) Macromolecules 34:6156
67. Jaeger R, Schönherr H, Vansco GJ (1996) Macromolecules 29:7634
68. Krause S, Dersch R, Wendorff JH, Finkelmann H (2007) Macromol Rapid Commun 28:2062
69. Ward IM, Sweeney J (2004) An introduction to the mechanical properties of solid polymers. Wiley, Weinheim
70. Thumser DA, Bergmann R (2005) Material Werkst 36:204
71. Gu S-Y, Wu Q-L, Ren J, Vansco GJ (2005) Macromol Rapid Commun 26:716
72. Bellan M l, Kameoka J, Craighhead HG (2005) Nanotechnology 16:1095
73. Lee SH, Tekman C, Sigmund WM (2005) Mater Sci Eng A 398:77
74. Zusssman E, Theron A, Yarin AL (2003) Appl Phys Lett 82:973
75. Li D, Wang Y, Xia Y (2003) Nano Lett 3:1167
76. Kameoka J, Craighead HG (2003) Appl Phys Lett 83:371
77. Sun D, Chang C, Li S, Lin L (2006) Nano Lett 6:839
78. Belardi J (2007) Diploma Thesis Marburg
79. Kidoaki S, Kwon IK, Matsuda T (2004) Biomaterials 26:37

80. Fagerlund G (1973) Determination of specific surface by the BET method. Springer, Dordrecht
81. Tomadakis MM, Sitirchos SV (1991) AIChE J 37:74
82. Tomadakis MM, Sitirchos SV (1993) AIChE J 39:397
83. Tomadakis MM, Sitirchos SV (1993) J Chem Phys 98:616
84. Tomadakis MM, Sitirchos SV (1991) AIChE J 37:1175
85. Gorham WF (1964) J Polym Sci A 1(4):3027
86. Hellen EKO (1997) J Appl Phys 81:6425
87. Maze B, Tafreshi VH, Wang Q, Pourdeyhimi B (2007) J Aerosol Sci 38:550
88. Matthews JA, Wnek G, Simpson DG, Bowlin GL (2002) Biomacromolecules 3:232
89. Placke D (2007) PhD Thesis, Philipps University, Marburg
90. Sun Z, Zussman A, Yarin AL, Wendorff JH, Greiner A (2003) Adv Mater 15:1929–1932
91. Reznik SN, Yarin AL, Zussman E, Bercovici L (2006) Phys Fluids 18:062101/01–062101/13
92. Yarin AL, Zussman E, Wendorff JH, Greiner A (2007) J Mater Chem 17:1–16
93. Greiner A, Wendorff JH, Yarin AL, Zussman E (2006) Appl Microbiol Biotechnol 71:387
94. Yu JH, Fridrikh SV, Rutledge GC (2004) Adv Mater 16:1562–156
95. Lopez-Herrera JM, Barrero A, Lopez A, Loscertales IG, Marquez M (2003) J Aerosol Sci 34:535–552
96. Hou H, Jun Z, Reuning A, Schaper A, Wendorff JH, Greiner A (2002) Macromolecules 35:2429–2431
97. Bognitzki M, Hou H, Ishaque M, Frese T, Hellwig M, Schwarte C, Schaper A, Wendorff JH, Greiner A (2000) Adv Mater 12:637–640
98. Caruso R, Schattka JH, Greiner A (2001) Adv Mater 13:1577–1579
99. Sun Z, Zeng J, Hou H, Wickel H, Wendorff JH, Greiner A (2005) Prog Colloid Polym Sci 130:15–19
100. Flory PJ (1969) Statistical Mechanics of Chain Molecules. Butterworth-Heinemann, London
101. de Gennes P (1980) Scaling Concepts in Polymer Physics. Cornell University Press, Cornell, NY
102. Larrondo L, Manley RS (1981) J Polym Sci Polym Phys 19:909
103. Kim JS, Lee D-S (2001) Polymer J 32:616
104. Lee S, Obendorf SK (2006) J Appl Polym Sci 102:3430
105. Dalton PD, Klinkhammer K, Salber J, Klee D, Möller M (2006) Biomacromolecules 7:686
106. M Becker (2006) PhD Thesis, Philipps University, Marburg
107. Stoiljkovic A, Ishaque M, Justus U, Hamel L, Klimov E, Heckmann W, Eckhardt B, Wendorff JH, Greiner A (2007) Polymer 48:3974
108. Matthews JA, Wnek GE, Simpson DG, Bowlin GI (2002) Biomacromolecules 3:232
109. Ohkawa K, Cha D, Kim H, Nishida A, Yamamoto H (2004) Macromol Rapid Commun 25:1600
110. Stephens JS, Fahnestock SR, Farmer RS, Kiick KL, Chase DB, Rabolt JF (2005) Biomacromolecules 6:1405
111. Zheng M, Skomski R, Liu Y, Sellmyer DJ (2000) J Phys Condens Mater 12:L497
112. Martin JI, Costa-Kramer JL, Briones F, Vicent JL (2000) J Magn Magn Mater 221:215
113. Sorop TG, Nielsch K, Göring P, Kröll M, Blau W, Wehrspohn RB, Gösele U, de Jongh LJ (2004) J Magn Magn Mater 272–276:1656
114. Graeser M, Greiner A, Wendorff JH (2007) Macromolecules 40:6032

115. Graeser M (2007) PhD Thesis, Philipps University, Marburg
116. Tan ST, Wendorff JH, Pietzonka C, Jia ZH, Wang GQ (2005) ChemPhysChem 6:1461
117. Wang M, Singh H, Hatton TA, Rutledge GC (2004) Polymer 45:5505
118. Bognitzki M, Becker M, Graeer M, Massa W, Wendorff JH, Schaper A, Weber D, Beyer A, Gölzhäuser A, Greiner A (2006) Adv Mater 18:2384
119. Graeser M, Greiner A, Pietzonka C, Massa W, Wendorff JH (2007) Adv Mater 19:4244
120. Schreuder-Gibson HL, Gibson P, Senecal K, Sennett M, Walker J, Yeomans W, Ziegler D, Tsai PP (2002) J Adv Mater 34:44
121. Gibson P, Schreuder-Gibson H, Rivin D (2001) Colloid Surf A 187/188:469
122. Hajara MG, Metha K, Chase GG (2003) Sep Filtr Technol 30:74
123. Maze B, Vahedi Tafreshi H, Wang Q, Pourdwyhimi B (2007) J Aerosol Sci 38:550
124. Stasiak M, Röben C, Rosenberger N, Schleth F, Studer A, Greiner A, Wendorff JH (2007) Polymer 48:5208
125. Berghoef MM, Vansco GJ (1999) Adv Mater 11:1362
126. Boudriot U, Dersch R, Greiner A, Wendorff JH (2006) Artif Org 30:785
127. Boland ED, Wnek GE, Simpson DG, Palowski KJ, Bowlin GL (2001) J Macromol Sci Pure Appl Chem 38:1231
128. Sanders EH, Kloefkorn R, Bowlin GL, Simpson DG, Wnek GE (2003) Macromolecules 36:3803
129. Zeng J, Aigner A, Czubayko F, Kissel T, Wendorff JH, Greiner A (2005) Biomacromolecules 6:1484
130. Timbrell V (1965) Ann NY Acad Sci 132:255
131. Harris RL, Fraser DA (1976) Am Industr Hygien Assoc J 37:73